Iron Oxide Fe3O4 Nanoparticles with Intrinsic Conducting Polymers and Biochar to Improve the Electromagnetic Shielding Performance of Light Weight Absorption-Type Materials

(Article begins on next page)

28 April 2024

# Iron Oxide Fe$_3$O$_4$ Nanoparticles with Intrinsic Conducting Polymers and Biochar to Improve the Electromagnetic Shielding Performance of Light Weight Absorption-Type Materials

## Amelia Carolina Sparavigna[1]

[1]Department of Applied Science and Technology, Polytechnic University of Turin, Italy

**Abstract**: Magnetic iron oxide nanoparticles (Fe$_3$O$_4$) can be dispersed in a supporting material so that the composite can better respond to electromagnetic fields, absorbing a part of their energy. In the discussion here proposed we will consider the role of these nanoparticles in applications for electromagnetic interference (EMI) shielding. Inserted in intrinsically conducting polymers (ICPs) for instance, the nanoparticles are increasing EMI shielding effectiveness of polymer, producing light weight "absorption-type" shields, which are specifically relevant for absorbing microwaves. Encapsulation of Fe$_3$O$_4$ nanoparticles with polypyrrole and polyaniline will be described in detail and the recent biochar-based composites, Fe$_3$O$_4$@biochar, will be discussed too.

**Keywords:** Magnetic iron oxide nanoparticles, Fe$_3$O$_4$, Magnetite, Electromagnetic interference shielding effectiveness, EMI-SE, Reflection loss, Microwaves absorption, Intrinsically conducting polymers, Polypyrrole, Polyaniline, EMI shielding textiles, Biochar

## Introduction

Electromagnetic shielding applications are relevant to protect human health and electronic devices against dangerous effects of electromagnetic radiations (Sparavigna et al., 2005). Metals are usually considered the best materials for electromagnetic shields, due to their peculiar ability in reflecting the electromagnetic waves. Metals or metal-coated materials generally show a very high electromagnetic interference shielding effectiveness EMI-SE, because their high conductivity makes them shield by surface reflection (Henn & Silverman, 1991, Henn & Cribb, 1983). However, metals and metal-coated materials cannot be used as electromagnetic wave absorbers. Materials, such as intrinsically conducting polymers (ICPs) can absorb as well as reflect electromagnetic waves, and exhibit certain advantages over metallic materials, such as easy preparation, light weight, good environmental resistance (Soares et al., 2021). The most prominent ICPs for EMI-SE are polypyrrole PPy and polyaniline PANI, where electrical conductivity can have values comparable to those observed for poorly conducting metals and alloy.

We considered ICPs for EMI shielding (Avloni et al., 2006), particularly PPy in composites for woven and non-woven fabrics (Avloni et al., 2007, 2008), mentioning the importance of the absorption of radiation. In fact, absorption of textiles with PPy is in percentage relevant: it was measured to be four times that of metallized fabrics (see Avloni et al., 2007, for details). As given by further research , the use of specific nanoparticles can relevantly increase the intrinsic EMI absorption mechanism of ICPs, producing in this manner light weight "absorption-type" shielding materials, today specifically investigated to obtain microwave absorption. Due to the use of electromagnetic waves in the GHz range for mobile phone and radar systems, microwave absorbing materials are regarded as very attractive. Moreover, these materials have also the specific significance of protecting humans and electronic devices against the secondary electromagnetic pollution produced by radiation reflected from metallic surfaces.

To prepare an absorption-type shielding material, suitable permittivity and permeability are required, accompanied by a finite electrical conductivity. As told by Arora et al., 2014, particles possessing high dielectric constant like ZnO, SiO$_2$, TiO$_2$, BaTiO$_3$, or high magnetic permeability like carbonyl iron, Ni, Co, Fe metals, $\gamma$-Fe$_2$O$_3$, Fe$_3$O$_4$, are used as fillers in polymeric materials to increase their shielding performance. Responding to an external magnetic field, these particles, such as the magnetite Fe$_3$O$_4$ nanoparticles, are able of absorbing its energy (Ni et al., 2009).

✏ **Amelia Carolina Sparavigna (Correspondence)**
☏ +

As we will deduce from literature, magnetite $Fe_3O_4$ nanoparticles are suitable for obtaining absorbing EMI shielding composites, based on several different supporting materials, ranging from commercial polymers to eco-friendly materials, such as the more recently considered biochar, for instance. Biochar is remarkable for its hierarchical porous structure (Sparavigna, 2023), and nanoparticles can be easily inserted in its pores to decorate the surface, enhancing its intrinsic EMI shielding features. Besides stressing the use of magnetite in biochar, the discussion will also provide some literature about the microscopic mechanisms which are producing the effective permittivity and permeability of materials. We will also see that several researchers are stressing that the different absorbing mechanisms of nanoparticles and supporting materials are acting synergically in improving the shielding effectiveness.

For what regards the composites with ICPs we will start from the analysis of $Fe_3O_4$ with PPy, but before, some words about shielding effectiveness and reflection loss, and about the magnetite nanoparticles in the form of core-shell particles are necessary.

Previous layout, February 23, 2023, of the discussion here proposed is available at SSRN, https://papers.ssrn.com/sol3/papers.cfm?abstract_id=4331866 . The layout of January 24, 2023, is available at ChemRxiv, link https://doi.org/10.26434/chemrxiv-2023-g9bkz-v2 .

**Reflection loss**
As we will see, in literature we can find the absorption performance of a shield given as SE, that is shielding effectiveness, or as RL, reflection loss. About the definition of the reflection loss, a discussion is given by Poplavko, 2021. Poplavko considers that the microwave-absorbing process is combining large losses and low reflection. As a rule, the microwave absorbing materials are made of polymer or rubber with fillers, which are conductive, magnetic or high-loss dielectric materials. In nonmagnetic material, the dissipation of energy is a result of dielectric relaxation and conduction mechanisms, that is through damping forces acting on the polarized atoms and molecules, and through the finite conductivity of a material. In the magnetic materials, according Poplavko, microwave absorption happens when the energy of spin waves is partially transferred to acoustic vibrations of the crystal lattice through spin-lattice interaction.

Simple EM analyses are made in two manners, by means of a microwave-shielding layer (SL) or by a microwave-absorbing covering (MA). Both are considered in normal incidence and transmission through a single absorbing layer.
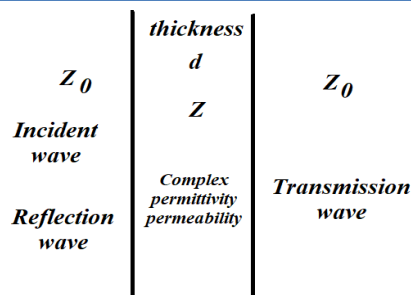


*Fig.1: Here we reproduce schematically the Fig. 5.1 of Poplavko's book. The image is giving the shielding layer with a thickness d.*

In the case of a shielding layer, one of the relevant parameters is the impedance. $Z = Z_0(\mu*/\epsilon*)^{1/2}$, with $Z_0$ being the vacuum impedance. Here we can find the complex relative permittivity and the complex relative permeability $(\epsilon*, \mu*)$ of the shielding material. In nonmagnetic media: $Z = Z_0/(\epsilon*)^{1/2}$ . Let us introduce $\gamma = i\omega (\epsilon*)^{1/2}/c$, being $\omega$ the circular frequency and $c$ the speed of light.

The absorption EM wave in nonmagnetic material is characterized by the attenuation coefficient (see Poplavko, 2021):

$$\alpha = \frac{\omega}{c}\sqrt{\frac{1}{2}\Re(\epsilon*)(\sqrt{1+\tan^2\delta}-1)}$$

Here we have: $\tan\delta = \Im(\epsilon*)/\Re(\epsilon*)$. Using this parameter, we can find the part of the shielding effectiveness coming from absorption, $SE_A = 8.686\alpha d$, where $d$ is the thickness of the absorbing layer. The shielding effectiveness is the sum of contributions coming from reflection, absorption, and multiple reflections: $SE = SE_R + SE_A + SE_{MR}$.
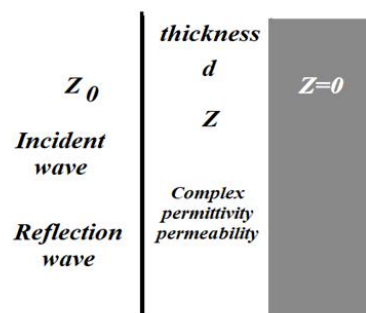


*Fig. 2: Here schematically the Figure 5.3 of the Poplavko's book. The absorbent layer is over a perfect conductor (PEC condition), with assumed zero impedance.*

The complex reflection coefficient is defined as: $\rho = \frac{Z_{in}-Z_0}{Z_{in}+Z_0}$, where $Z_{in}$ is the input impedance, obtained from the long transmission lines theory (Prokopchuk et al., 2021).
The reflection loss is given by:

$$RL = 20\log_{10}\left(\frac{\sqrt{\mu*}\tanh(\gamma d)-\sqrt{\epsilon*}}{\sqrt{\mu*}\tanh(\gamma d)+\sqrt{\epsilon*}}\right).$$

For nonmagnetic media:

$$RL = 20\log_{10}\left(\frac{\tanh(\gamma d) - \sqrt{\epsilon^*}}{\tanh(\gamma d) + \sqrt{\epsilon^*}}\right).$$

Microwave absorption efficiency is given by: $MA = -RL$.

In Ramo et al., 1994, Micheli et al., 2010, by means of the analogy with the transmission line, the input impedance of the layer (air/absorber interface) is given as:

$$Z_{\text{in}} = \eta \frac{Z_L\cos(\zeta d) + j\eta\sin(\zeta d)}{\eta\cos(\zeta d) + jZ_L\sin(\zeta d)}$$

Here $\eta = Z_0/\sqrt{\epsilon^*}$, $\zeta = -j\gamma$. $Z_L$ is the "load" of the line. In the case it is negligible (PEC condition as in the figure), we have:

$$Z_{\text{in}} = jZ_0 \frac{1}{\sqrt{\epsilon^*}}\tan(\zeta d) = Z_0 \frac{1}{\sqrt{\epsilon^*}}\tanh(\gamma d)$$

The reduced impedance is given by:

$$\tilde{Z}_{\text{in}} = \frac{1}{\sqrt{\epsilon^*}}\tanh\left(j\frac{\omega d}{c}\sqrt{\epsilon^*}\right),$$

as in Du et al., 2014. And the reflection loss in Chakradhary et al., 2020:

$$RL(dB) = 20\log_{10}\left|\frac{\tilde{Z}_{\text{in}} - 1}{\tilde{Z}_{\text{in}} + 1}\right|$$

As told by Micheli et al., 2010, the "absorption capability" of a layer is coming from "both dielectric losses within the material and impedance matching condition". As stressed by Micheli et al., when the imaginary part of $Z_{\text{in}}$ vanishes for multiple values of the quantity $\zeta d$, and if the real part of $Z$ is close to $Z_0$ we have the "matching condition" to find RL going to minus infinity. Specifically, when the thickness of the layer is an odd multiple of the quarter wavelength in the composite (nonmagnetic medium):

$$d = n\frac{\lambda}{4} \text{ with n=1,3,5, ... and } \lambda = \frac{c}{2\pi}\frac{\omega}{\sqrt{|\epsilon^*|}}$$

Therefore, "the incident and reflected waves are out of phase, thus giving no reflection at the air-absorber interface" (Micheli et al., 2010). Let us consider all in more detail.

If the thickness of the absorber layer satisfies the equation given above, we have, as told by Deng and Han, 2007, that the electromagnetic wave EW can be "absorbed" through a "geometrical effect". Deng and Han mention this geometrical effect also reported by Yusoff et al., 2002, in LiNiZn ferrite/thermoplastic natural rubber composites. At specific thicknesses, "the incident and reflected waves in the material are out of phase 180°, resulting in total cancellation of the reflected waves at the air–material interface" (Yusoff et al., 2002). This phenomenon is also known as "quarter-wavelength attenuation". Chen et al., 2020, explain that it is occurring because the microwave reflected by the surface of the perfect conductor and "the microwave reflected on the top of sample are out of phase by 180° at the air-absorber interface". The phase difference produces a "partial interference cancellation and a decline in reflection" (Chen et al., 2020).

Let us consider the work by Yusoff and coworkers on ferrite composites. The researchers assume the absorption characteristics of their samples in normal incidence of TEM wave in the model based on a single-layered plane wave absorber backed by a perfect conductor. The ferrite resulted as a narrowband absorber, whereas the polymeric material has a broadband absorption characteristic. "Minimal reflection of the microwave power or matching condition occurs when the thickness of the absorber approximates an odd number multiple of a quarter of the propagating wavelength" (Yusoff et al., 2002). Li–Ni–Zn ferrite exhibits another matching condition at low frequency, given by $|\mu^*| = |\epsilon^*|$.

The reflection coefficient given by Yusoff and coworkers is:

$$\Gamma = (Z_{\text{in}}/Z_0 - 1)/(Z_{\text{in}}/Z_0 + 1)$$
$$= \frac{[(\mu^*/\epsilon^*)^{1/2}\tanh(\gamma d) - 1]}{[(\mu^*/\epsilon^*)^{1/2}\tanh(\gamma d) + 1]}$$
$$\text{with } \gamma = \frac{j\omega\sqrt{\mu^*\epsilon^*}}{c}.$$

Besides the matching of impedance for quarter-wave geometrical effect, Deng and Han note that when an electromagnetic wave is incident on an absorber, to have zero reflection the absorber relative permeability and relative permittivity must be $\mu^* = \epsilon^*$. In the case of the composites studied by Deng and Han, which are containing multi-walled carbon nanotubes, permittivity is "much larger than" permeability. The impedance matching condition $\mu^* = \epsilon^*$ "cannot be satisfied. ... the observed microwave absorbing performance ... is due to the geometrical effect". Actually, we have two matching conditions, one concerning the quarter-wave, the other the relative permittivity and permeability of the absorbing medium at air interface.

Here, it is necessary to add reference to the work by Liu et al. (2021, 2022), regarding the investigation on the quarter-wavelength model. Liu and coworkers are stating that the model consists in microwave reflection minimization, when the "thickness of the film is $m\lambda/4$ where $m$ is an odd integer and $\lambda$ is the wavelength within the film" (Liu et al., 2022). In their work of 2021, Liu and coworkers say that many concepts "in current *mainstream* microwave absorption theory are used inappropriately including that reflection loss RL", and "the results have been rationalized incorrectly by impedance matching theory. Impedance matching theory is developed from transmission-line theory for scattering parameter s₁₁ but cannot be applied to RL which is an innate property only for metal-backed film" (Liu et al., 2022).

**Peak frequency of microwave absorption**
Wang et al., 2011, investigated the peak frequency of microwave absorption in the case of carbonyl iron/epoxy resin composite. The introduction explains the reason for investigating RL of materials. Wang and coworkers are precisely telling that "The applicability of a microwave absorption material has been based on the fact that there is one maximum microwave

absorption or a dip in reflection loss (RL) in the desired frequency range". The "dip" in RL, that is its going down to a lower level, "is equivalent to the occurrence of minimum reflection loss for the incident microwave power at a particular thickness" (Wang and coworkers are mentioning Yusoff et al.). Among the parameters used to characterize the microwave absorber, the "peak frequency of the dip is the most crucial parameter". In fact, if the peak frequency of the dip is away from what we need, "even an excellent microwave absorbing capability seems useless" (Wang et al., 2011).

Wang and coworkers told in 2011 that various models have been proposed to give the frequency of the dips in RL, but two of them are more used: the model by Naito and Suetake, 1971, and the quarter-wavelength condition, that we have previously discussed.

$$t_m = \frac{c}{\omega_m \Im(\mu^*)} \text{ (Naito \& Suetake, 1971)}$$

$$t_m = \frac{nc2\pi}{4\omega_m\sqrt{|\epsilon^*\mu^*|}} (n=1,3,5,...) \text{ (quarter-wavelength)}$$

where $t_m, \omega_m$ are the *matching layer thickness* and *peak angular frequency* at the dip.

Wang and coworkers evaluate RL for carbonyl iron/epoxy resin composites. For the different samples that have been investigated, the researchers conclude that the reflection loss is complying with the quarter-wavelength condition (Wang et al., 2011).

Just to illustrate the dips of RL, let us consider a nonmagnetic layer, thickness 3 mm. Here in the following figure, the behavior of RL (dB) as a function of the frequency in the case of $\epsilon^* = 10 - j1.8$, with $j^2 = -1$.
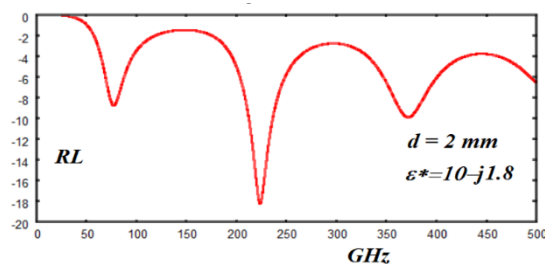


*Fig. 3: An example of reflection loss at given values of thickness and complex permittivity.*

**Fe₃O₄ and magnetic loss**
In Yang et al., 2020, we can find preparation of Fe₃O₄ and a study of its absorption properties. The prepared sample had 40% mass fraction of ferrite particles mixed with paraffin. The Fe₃O₄ particles were obtained by chemical precipitation-dehydration, from ferrous chloride and ferric chloride as iron sources, SEM analysis shows particles with rough and uneven surface, irregular circular shape with a diameter of about 1-3 μm. Yang and coworkers identify the magnetic loss of Fe₃O₄ in hysteresis, eddy current loss and natural resonance in the range from 2 to 18 GHz.

However, hysteresis is negligible under weak magnetic field.
The researchers provide a relation for the imaginary part of the permeability: $\Im(\mu^*)/\mu_0 \approx \omega(\Re(\mu^*)\mu_0)^2\sigma\, d^2/3$, where $d$ is the diameter and $\sigma$ the conductivity of the metal particles, and $\mu_0$ the vacuum permeability. Accordingly, the magnetic loss of the absorbing material, which is related to the imaginary part of the permeability, depends on the diameter and conductivity of the particles.

In Yang et al. 2020, we can find an example of evaluation of RL in the case of a composite made of Fe₃O₄ micron-size particles and paraffin. Let us now consider how to reduce Fe₃O₄ particles in nanoparticles.

**Fe₃O₄ nanoparticles production**
In Blaney, 2007, we can find the detailed description of magnetite (Fe₃O₄). A section of the article explores the bulk properties of it. For the electrical properties, the conductivity ranges from $10^2$–$10^3$ $\Omega^{-1}cm^{-1}$ (Cornell & Schwertmann, 1996). This electrical conductivity is evidencing a semi-conductor behavior, bordering the conductor (metallic) behavior. A semi-metallic behavior is further supported by magnetite relatively low bandgap (0.1 eV) (Cornell & Schwertmann, 1996). The Curie temperature is at 850 K. Below the Curie temperature, magnetite is a ferrimagnetic material (Cornell & Schwertmann, 1996). When the Curie temperature is attained, a superparamagnetic behavior is observed.

If we consider the particles, as the particle size decreases, the behavior tends towards a paramagnetic or super-paramagnetic magnetization. Therefore, the decreasing of the particle size reduces ferrimagnetic behavior and enhances superparamagnetic behavior (Blaney, 2007). The Curie temperature is affected by the particle size; since the superparamagnetic magnetism is observed at room temperature, the effective Curie temperature of the nanoparticles must be lower than that of the bulk material (Blaney, 2007).

In his article, Lee Blaney gives a detailed discussion of the nanoparticle synthesis techniques. Most of these techniques falls under two categories: polymer/surfactant assisted precipitation reactions and co-precipitation reactions. One of the surfactant assisted reaction is the reverse micelle method. It is based on a water-in-oil emulsion that generates reverse surfactant micelles. The hydrophilic cores of reverse micelles are nanoreactors for various processes. Metal species can be dissolved into the aqueous phase contained within the reverse micellar cores. In this manner a nanoreactor is obtained, having the species of interest at the reverse micelle center. Simultaneous production and steric stabilization of the nanoparticles can be realized.

For $Fe_3O_4$ the following procedure reported by Blaney is that given by Lee et al., 2005, who have detailed a protocol to prepare nanoparticles of uniform diameters over the 2-10 nm range. The particle size is given by the relative amounts of surfactants, solvents, and polar solvents. The used surfactant is the dodecyl-benzene-sulfonate. It is added to an oil (xylene) solution. The emulsion solution is mixed by sonication. An iron solution with 1:2 (molar ratio) of ferrous chloride and ferric nitrate in ethanol is then vigorously stirred into the emulsion solution. In a few seconds, the emulsion becomes transparent and after stirring for 12 hours, the reverse micelle phase, that is the water-in-oil phase, is stabilized. Then a gradual heating of the phase to 90 °C in argon flow ensues. Hydrazine is added to the system and immediately the transparent solution becomes black. Refluxing and centrifugation in ethanol recover the magnetite nanoparticles.

$Fe_3O_4$ nanoparticles are sometimes mentioned as MIONs (Monocrystalline Iron Oxide Nanoparticles), or designed as iron oxide NPs (IONPs), and because of their super-paramagnetic (SPM) behavior SPM IONPs or SPIONs (Wallyn et al., 2019). Dispersed in a supporting material, they can respond to an external magnetic field (Tong. et al., 2019).

**Ferric Nitrate, that is, Iron Nitrate**
We have previously mentioned the Ferric Nitrate. Iron(III) nitrate, that is the ferric nitrate, is the name addressing a family of inorganic compounds with formula $Fe(NO_3)_3.n(H_2O)$. The most common member

of the family is the nonahydrate $Fe(NO_3)_3.(H_2O)_9$ (nona=9). The compounds can be prepared by treating iron metal powder with nitric acid.

Rarely, we find the ferric nitrate mentioned as "iron nitrate". For instance, the "iron nitrate heptahydrate $(Fe(NO_3)_3.7H_2O)$" (hepta=7) has been used for a "simple hydrothermal co-precipitation and calcination-free method to synthesize a cobalt ferrite-based Fenton-like catalyst for the degradation of organic wastewater" (Shi et al., 2022). The final product was $CoFe_2O_4$. In Li et al., 2022, for the Fenton-like catalyst preparation too, we find written "ferric nitrate heptahydrate $(Fe(NO_3)_3.9H2O)$". But this is the nonahydrate, not the heptahydrate.

Merck, via the web site of Sigma-Aldrich, https://www.sigmaaldrich.com/IT/it/substance/ironiii nitratenonahydrate404007782618 , is providing nonahydrate with the name Iron(III) nitrate nonahydrate, synonyms ferric nitrate nonahydrate, Iron(III) nitrate nonahydrate. The heptahydrate seems being not available through Sigma-Aldrich.

In Le Bolay et al., 2020, for the production of hematite micro- and nanoparticles, the iron nitrate $Fe(NO_3)_3.9H_2O$, purchased from Sigma Aldrich France, was used as precursor. The researchers obtained the ferric nitrate *heptahydrate* $Fe(NO_3)_3.7H_2O$ by heat treatment of solution in a muffle furnace and in a lab convective dryer.
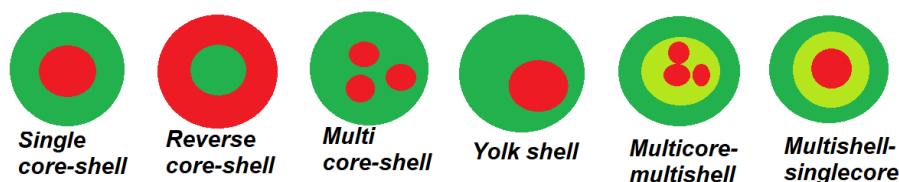


*Fig.4: Classification of core–shell nanostructures as proposed by Singh and Bhateria (2021).*

**Fe₃O₄@C: a core-shell model**
About the absorbing EMI shielding composites, we can find in literature that several researchers are stressing that the different absorbing mechanisms of nanoparticles and supporting materials are acting *synergically* in improving the shielding effectiveness.

To have the synergy, $Fe_3O_4$ nanoparticles are encapsulated in carbon or polypyrrole. In the article by Du et al., 2014, we can find investigated the microwave absorption of core–shell $Fe_3O_4$@C composites. It is stressed that $Fe_3O_4$ and carbon composites have received much attention because of the "tunable properties and highly chemical stability of carbon materials" and for a "significant *synergetic or complementary* behavior" of $Fe_3O_4$ and carbon (Du et al., 2014). The researchers consider that the construction of core−shell structures is a good route to

improve the functionality of composites. We have spheres with a $Fe_3O_4$ core covered by a carbon shell, therefore we have an encapsulation which is properly indicated by @ in the $Fe_3O_4$@C composite name. However, symbol @ is not only used to represent an encapsulation. It is also proposed for other composites, to indicate that the nanoparticles are inserted in a supporting material, for instance in graphene ($Fe_3O_4$@graphene, Yao et al., 2012), or used to decorate biochar ($Fe_3O_4$@biochar, Wang et al., 2022).

Once $Fe_3O_4$ spheres were prepared, they were coated by a shell with an in-situ polymerization and a high-temperature carbonization. A "typical recipe" is given by Du et al., 2014. The recipe starts from $Fe_3O_4$ microspheres dispersed in a solution, containing water, absolute ethanol, and ammonia. To the solution, mixed and treated by ultrasonication, resorcinol is

added and the mixture stirred, before adding formaldehyde to start polymerization. In this manner, $Fe_3O_4$@phenolic resin composites had been obtained, which were collected by magnetic separation. After suitable treatments, the $Fe_3O_4$@phenolic resin composites were carbonized.

In their article, Du and coworkers note that the microwave absorption properties are linked to the complex permittivity and permeability of the material. As we can find told in all literature about absorption of electromagnetic waves, the real parts of permittivity ($\varepsilon'$) and permeability ($\mu'$) are representing "the storage capability of electric and magnetic energy ... , and imaginary parts ($\varepsilon''$ and $\mu''$) stand for the loss capability of electric and magnetic energy" (Du et al., 2014). The measurements made by the researchers provided a poor dielectric loss of $Fe_3O_4$ microspheres, but the increase of carbon content was enhancing both $\varepsilon'$ and $\varepsilon''$. The enhancement can be attributed, according to Du and coworkers, to the higher electrical conductivity of carbon shell with respect to that $Fe_3O_4$ microspheres (see Du et al., 2014, and references therein).

Du and coworkers provide data about permittivity and permeability; $Fe_3O_4$ microspheres has "some magnetic loss abilities", but the imaginary part of permittivity is too low to produce a proper reflection loss RL. The increase of the thickness of the carbon shell is improving the complex permittivity, so that an effective characteristic impedance is obtained (Du et al., 2014). Consequently, the complex permittivity of $Fe_3O_4$@C has to be controlled in a rational manner.

**$Fe_3O_4$@polypyrrole and EMI absorption**
In Deng et al., 2003, we can find how to prepare core-shell $Fe_3O_4$–polypyrrole nanoparticles, that is $Fe_3O_4$@PPy. Before the proposal of this kind of particles, polypyrrole and magnetite composite films had been developed by Yan et al., 2001. Deng and coworkers prepared a "$Fe_3O_4$ magnetic fluid" by a precipitation–oxidation method. The starting mixture is of PEG and $FeSO_4 \cdot 7H_2O$ dissolved in water. After the method described in the article, the magnetic fluid was obtained and used for in situ emulsion polymerization in aqueous solution and NaDS. Water and NaDS are placed in a flask, stirred, and magnetic fluid added and stirred. Then, pyrrole is added and all stirred. The polymerization is started by adding drop-wisely $FeCl_3$ dissolved in water. After the polymerization and further procedures, $Fe_3O_4$–polypyrrole nanoparticles with core-shell structure are obtained. The transmission electron microscopy images of $Fe_3O_4$ and $Fe_3O_4$–polypyrrole particles show spherical particles with sizes ranging from 20 to 30 nm and 30 to 40 nm, respectively. The composite has been investigated by IR, UV–visible and X-ray photoelectron spectroscopy (XPS) spectra. In the

article by Deng and coworkers, no mention to EMI shielding or to microwave absorption is given.

Dey et al., 2005, considered the polymerization of pyrrole in the presence of nanoparticles of $Fe_3O_4$ with ammonium peroxodisulphate (APS) as oxidant. Dey and coworkers characterized the nanocomposites, finding that the magnetization data at room temperature show a small hysteresis loop. The Mössbauer spectra confirm the super-paramagnetic phase in magnetite. The composites have a semiconducting behavior, with polypyrrole ruling the transport process. "A very large dielectric constant of about 11 000 at room temperature has been observed. The interface between polypyrrole and $Fe_3O_4$ plays an important role in producing a large dielectric constant in the composite" (Dey et al., 2005).

Li et al., 2011, have proposed the synthesis of $Fe_3O_4$@PPy core/shell nanocomposites, where $Fe_3O_4$ nanoparticles are used as seeds for in situ polymerization on them. Li and coworkers measured the complex permeability and permittivity of the related composite materials to evaluate their microwave absorption properties. For measurements, the $Fe_3O_4$@PPy nanocomposites were mixed with paraffin wax. The real parts of complex permittivity and permeability represent - Li et al. are explaining - the storage of electric and magnetic energy, while the imaginary parts "symbolize the loss of electric and magnetic energy".

"Compared to other microwave absorption materials", the imaginary permittivity is higher (Li et al., 2011). "This phenomenon may result from the PPy shell due to its dielectric loss at high frequencies", and Li and coworkers stress that it is caused by the core/shell structure which produces an additional *interface with an interfacial polarization* at the surface of nanoparticles. The resulting higher imaginary part of permittivity means an increase of dielectric loss so that "more electromagnetic energy transfer into heat energy" (Li et al., 2011).

Guo et al., 2017, have proposed epoxy composites with polypyrrole functionalized nano-magnetite ($Fe_3O_4$@PPy), which have "significantly enhanced electromagnetic wave absorption performance and flame retardancy". The epoxy/(30.0 wt%)$Fe_3O_4$–PPy composites have a minimum reflection loss (RL) value of -35.7 dB. This value is much lower than that of epoxy/(7.5 wt%)PPy composite or epoxy/(30.0 wt%)$Fe_3O_4$ at the same thickness (1.7 mm). "The increased interface area, eddy current loss and anisotropic energy are essentially important to achieve higher reflection loss and broader absorption bandwidth" (Guo et al., 2017).

Wu et al., 2017, proposed a facile preparation of core–shell $Fe_3O_4$@PPy composites. The preparation is

based on a sequence of processes: etching, polymerization, replication. A reflection loss of −41.9 dB (that is >99.99% absorption) at 13.3 GHz, and matching layer thickness of 2.0 mm was achieved. "In comparison with other conductive polymer-based core–shell composites reported previously, the Fe₃O₄@PPy composites in this study" - Wu and coworkers are telling - "not only possess better reflection loss performance but also demonstrate a wider effective absorption bandwidth (<−10.0 dB) over the entire Ku band (12.0–18.0 GHz)" (Wu et al., 2017).

More recently, in 2020, Liu and Liao proposed again Fe₃O₄ nanoparticles and polypyrrole for preparing absorption-type electromagnetic interference shields and devices for radar stealth. Like Li et al, 2011, Liu and Liao consider the synergy related to electric and magnetic dipoles. They used Fe₃O₄ nanoparticles with polypyrrole (PPy) coating, fixed onto collagen fibers (CFs). For the synthesis of $CF_{0.5}Fe_3O_{4x}PPy_y$ composite, Liu and Liao used CFs and Fe₃O₄ NPs, immersed in an ethanol solution. Stirring the solution, the CF/Fe₃O₄ composite was obtained. Then Py monomer was added to the solution and the reaction initiated by $FeCl_3 \cdot 6H_2O$ in HCl. After the procedure detailed by the researchers, the final composite was obtained, where Liu and Liao inserted in the scaffold of the porous collagen microfibrils, a high loading of "magnetic-loss-activated" Fe₃O₄ nanoparticles separated inside the pores, then coated by a "dielectric-loss-activated" shell of polypyrrole. Measurements made by researchers show that the incident EMI energy can be dissipated by the already mentioned dielectric and magnetic losses and interfacial polarization loss (Liu & Liao, 2020). The hierarchical structure of the assembly of collagen fibers is characterized by pores from the nano- to the microscale, that are producing multiple reflection and scattering of waves. The porosity is therefore improving the attenuation capacity produced by Fe₃O₄ and PPy. The researchers are giving for their composites an EMI-SE value of ~72.0 dB, with an absorption contribution of 85.8%, with high radar-stealth performance (8.2–11.5 GHz).

As stressed by Liu and Liao, the impedance matching is a determinant feature for absorptive shielding material. In Li et al., 2017, for Co@C composites, we can find impedance matching and microwave attenuation too. By means of "moderate electromagnetic parameters", the composite material can have impedance matching together with attenuation ability. "Using magnetic/dielectric composites is considered to be an efficient strategy for achieving excellent electromagnetic absorbing properties" (Li et al., 2017).

Liu and Liao show that the increase in the composite of the presence of Fe₃O₄ nanoparticles NPs improves the magnetic properties, favoring the EMI dissipation through the resonance loss and eddy current loss (Wen, et al., 2011). The use of magnetic Fe₃O₄ NPs "*easily* realized the impedance matching between the shield and free space" (Liu & Liao, 2020). For what concerns the reflection loss RL, Liu and Liao tell that "RL value smaller than −5.0, −10.0, or −20.0 dB indicated that more than 70.0%, 90.0%, or 99.0% of incident EMWs [electromagnetic waves] are absorbed. The minimum RL values of the five samples were around −5.0 dB with a thickness of 2.0 mm." (Liu & Liao, 2020).

**Microwave absorbing materials (MAMs)**
Adebayo et al., 2020, also stress the importance of new materials for microwave absorption (frequencies between 300 MHz and 300 GHz). For the novel microwave absorbing materials (MAMs), magnetite (Fe₃O₄) is "thoroughly investigated", because of its permittivity and permeability and proper magnetization and Curie temperature (Adebayo et al., 2020). Limiting factors exist, such as the weight and the impedance mismatch, but they can be circumvented passing to the nanoscale, with the creation of hierarchical frameworks, and using magnetite with other loss materials. The Fe₃O₄ nanoparticles are complemented in their MA role by the carbon-based materials, that is carbon fibers, carbon nanotubes, porous carbon and graphene. The conductive polymers (PPy, PANI) are also involved.
The article by Adebayo and coworkers is detailing the electromagnetic mechanism. Here we just remember that we need an impedance of the absorptive material close to that of vacuum (377 Ω) and a rapidly attenuation of the waves in the material. As previously seen, we need magnetic and dielectric loss ability. The reduction of the impedance mismatch is important because a high mismatch results in high reflection of waves. For this reason, the design of *multilayer* absorptive materials, which are able of avoiding reflection and absorbing the waves, operating in the bandwidth of microwaves, are investigated. As reported by Adebayo et al., Xu et al., 2015, solved the problem with a multilayer comprising of PANI and Fe₃O₄/PANI. They obtained maximum absorption of about 54 dB.

**Permittivity and permeability**
Materials are usually classified into conductors, semiconductors, and dielectrics. Focusing on dielectric materials, for their applications it is essential to know the dielectric constant, that is the real part of complex permittivity, and the loss tangent at the given operating conditions (Brodie et al., 2015). A dielectric is a material which is polarized under an electric field (dielectric polarization). The polarizability of the material is given by the permittivity, which is a complex number. Together with the magnetic permeability, permittivity is determining the EM field propagation in the material. As shown by Lifšits and

Pitaevskij, 1986, in alternating electromagnetic fields, permittivity and permeability are complex quantities with an imaginary part which is always different from zero, according to causality principle and thermodynamics principles.

Starting from Maxwell's equations, we can explain the dielectric properties of materials. According to Brodie et al., 2015, we have the complex permittivity given by:

$$\varepsilon_c = \varepsilon' - j\varepsilon'' = \varepsilon - j\frac{\sigma}{\omega},$$

where we find the real dielectric constant $\varepsilon$, the imaginary part expressed as a "conductivity" $\sigma$ of the dielectric and the angular frequency $\omega$ . About this form of proposing the imaginary part of the permittivity, in all the frequency domain, see please the discussion given in Lifšits and Pitaevskij, 1986, Chapter 9, page 392.

The real part of the permittivity is related to the amount of energy of the electrical field stored in the material. The imaginary part is related to the amount of energy loss. The loss tangent is:

$$\tan\delta = \frac{\varepsilon''}{\varepsilon'}.$$

As given by Lifšits and Pitaevskij (1986) and Boris Katsenelenbaum, 2006, in his book on high-frequency electrodynamics, the energy dissipation is related to the divergence of Poynting vector. We can obtain the heat produced at a local density rate, being proportional to the imaginary part of permittivity and permeability.

About the complex permittivity and permeability linked to losses in materials, let us consider some different manners in proposing the subject. Let us start from the discussion by Qin et al., 2022, about the dielectric loss mechanisms relevant for electromagnetic wave absorption. The review is providing a comprehensive summary on dielectric mechanisms, including dipolar polarization, defect related polarization, space charge and interfacial polarization and dielectric (conduction) loss.

To have a good electromagnetic wave absorber, the practice is to increase dielectric and magnetic losses, which are causing dissipation. As noted by Qin and coworkers, the dielectric losses are due to different mechanisms: for absorbers tailored in 2–18 GHz frequency range, we must consider dielectric conductivity and polarization due to the presence of dipoles, interfaces and defects. Other mechanisms, which are ionic, atomic and electronic polarizations are seldom involved because they are relevant in the range of $10^3$–$10^6$ GHz.

In the review by Qin and coworkers, it is stressed that composites use magnetic materials, that can provide magnetic loss, and high-conductive materials that provide conductive loss. Therefore we need what we

have already mentioned, that is, the *synergistic* presence of magnetic materials and carbonaceous materials, such as graphene or carbon nanotube or conducting polymers. Qin and coworkers are mentioning in particular the work by Ding et al., 2019, that "boosted" the interfacial polarization by means of a multi-core-shell with TiO₂, Fe₃O₄ and PPy, to improve microwave absorption MA. To have interfacial polarization, porous or hollow materials are used too (Qin et al., 2022). The review describes in detail dipole polarization, distinguishing between displacement polarization and orientation polarization. Qin and coworkers note that polar functional groups such as carbonyl and hydroxide radicals can contribute to dipolar energy losses. "Functional groups are rich in most carbonaceous materials including carbon fibers, carbon nanotubes, *biochar*, and graphene" (see Qin et al, 2022, and references therein). Moreover, to promote the dipolar polarization loss, a strategy is that of anchoring functional groups on the surfaces of absorbing materials.

As well known, conduction loss is caused by the electromagnetic wave propagation when its energy is converted into charge transport energy. Since conductive loss exists in materials with suitable conductivity, Qin and coworkers mention again the carbon materials and also the conducting polypyrrole and polyaniline. About the conductive loss, two models are mentioned. The first model is related to the charge migration, that is to the charge propagating in the medium, which can be a nanotube or a graphene layer for instance. The other model is that of the charge hopping. It refers to the charge transfer between the components of the composite, but also between interfaces or defects in the material (Qin et al., 2022). This model requires enough filling ratio of absorbing elements. When the conductive network condition is satisfied, we have hopping electrons in the network and the presence of micro-current in it.

Another review we can mention is that by Ganguly et al., 2018, about polymer nanocomposites for EMI shielding. Again, we can find that the presence of electric and magnetic dipoles "can help in absorption of the radiation by the shield". Materials with high permittivity, for instance BaTiO₃, are providing electric dipoles, whereas magnetic dipoles can be provided by Fe₃O₄ or other materials with high magnetic permeability.

In Ganguly et al., 2018, we can find mentioned the development of a high-performance shielding material in the form of polyaniline (PANI) based nanocomposite and Fe₃O₄ decorated graphite oxide (Singh et al. 2013). EMI-SE is of 26 dB at 15 GHz, with reflection loss of 6 dB. Another interesting work about Fe₃O₄ is that by Hosseini et al., 2011, who coated polythiophene nanofibers with MnFe₂O₄/Fe₃O₄

core–shell nanoparticles, synthesized with co-precipitation and in situ polymerization.

Kruželák et al., 2021, consider EMI-SE absorption of rubber composites based on ferrite and carbon fillers (carbon black and nanotubes). From experimental data, it is seen that the composites filled only with carbon black or carbon nanotubes have low real permeability and negligible imaginary permeability. This fact is displaying a non-magnetic character of carbon-based fillers. The incorporation of ferrite, that has magnetic dipoles, increases of complex permeability. The permeability is depending on "spin precession, domain wall movement, hysteresis loss and eddy current effect" (Kruželák et al., 2021). The hysteresis loss is negligible when low magnetic fields and high frequencies are involved. Spin precession and domain wall movement relate to resonance phenomena observed in the permeability spectrum. Eddy current effect might also contribute to permeability loss, relevant for small particles.

About the real part of the permittivity $\varepsilon'$, which is representing the "electrical charge storage capacity", it can be understood as simulated by micro-capacitors. "Micro-capacitors are formed by particles or aggregates of the fillers that act as electrodes filled with insulating rubber matrix" (Kruželák et al., 2021). Defects of the filler structure act as polarization centers. Therefore, the increase of the presence of micro-capacitors and structural defects produces an increase in real permittivity of composites. The increase of the filler loading reduces the gap between filler particles; this produces an increase of the polarization of the rubber matrix. In the case the concentration of fillers (conductive fillers) reaches the *percolation threshold*, there is the formation of filler conductive paths. The conductive filler networks are acting as dissipating mobile charge carriers too. In fact, several phenomena and related relaxations are influencing the permittivity. "Interfacial and space charge relaxations occur because charge carriers are trapped at the interfaces of heterogeneous composite system" (Kruželák et al., 2021).

For what is regarding the magnetic fillers, Ruiz-Perez et al., 2022, consider that an improvement of the "electromagnetic attenuation response" can be obtained through the insertion of super-paramagnetic materials. "Several strategies have been addressed to improve the dielectric properties of carbon-based polymer composites, including the hybridization with magnetic metals … [but] super-paramagnetic materials are the best option for microwave absorber

compounds". (Ruiz-Perez et al., 2022). Therefore, the Fe₃O₄ nanoparticles are interesting for microwave absorbers.

Wang et al., 2021, consider both the dielectric and the magnetic losses, besides the impedance matching condition, in their discussion about the progress of microwave absorption of materials by "magnetic–dielectric synergy". Under the "polarization loss", we can find that the loss is mainly due to dipole polarization and interface polarization. The dipoles are linked to "active sites", given by defects and surface functional groups. "When the carriers accumulated at the interfaces", we have generated the interfacial relaxation, which can dissipate the incident EM energy. Equivalent circuit models have been proposed for interfacial polarization. The proposed example is the peak at about 14.1 GHz for the imaginary part of the permittivity in the case of Fe₃O₄/ Carbon-Nanotubes hybrids, corresponding to the heterojunction capacitor produced by the interface between Fe₃O₄ and nanotubes.

About the "conduction loss", Wang and coworkers are mentioning the carbon-based materials and some polymer materials. Considering the "transmission line theory", the conductivity with electronic transport is proportional to the values of $\varepsilon''$ (Wang et al., 2021, Cao et al. 2012): in alternating EM fields, "some electrons" can "move directly", other electrons can "jump across the interface".

About the magnetic loss, when an EM wave enters the material, a dynamic magnetization process is created which is consuming energy. Thus, also in this case, the magnetic permeability is expressed as $\mu = \mu' - j\mu''$, where real $\mu'$ and imaginary $\mu''$ parts of permeability are depending on frequency. Wang and coworkers note that the frequency range can be subdivided into some main regions. In the low frequency region, less than $10^6$ Hz, the values of $\mu'$ and $\mu''$ change little. In the frequency range ($10^6$–$10^8$ Hz), $\mu'$ is rapidly decreasing, whereas $\mu''$ has a peak, mainly due to the resonance of magnetic domain walls. In the range $10^8$–$10^{10}$ Hz, natural resonance is occurring. When the frequency is greater than $10^{10}$ Hz, we have the ferromagnetic resonance. "Magnetic loss mainly includes hysteresis loss, domain wall resonance, natural resonance, ferromagnetic resonance and eddy current loss" (Wang et al., 2021). The natural resonance is that which appears at the frequency of precession of magnetic moments in the material (Sabu et al., 2012).
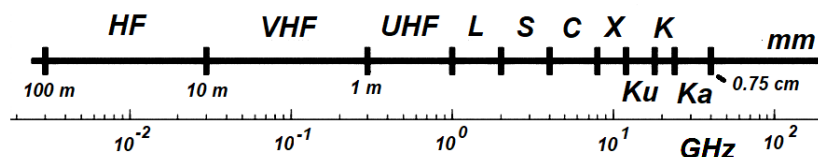
*Fig. 5: Frequency bands, as given by Etienne Everaere, E. (2015).*

### Fe₃O₄@Graphite

Wang et al., 2022, have proposed Fe₃O₄–Graphite composites as MAMs. In their approach, electromagnetic features and impedance matching were regulated by the graphite percentage. The optimal ratio for bimodal performance is 3:10 (Fe₃O₄–2PG, Pre-treated Graphite). With a thickness of 4 mm, the minimum reflection loss $RL_{min}$ in C-band (4–8 GHz) was measured as −40.6 dB, and $RL_{min}$ in Ku-band (12–18 GHz) was −29.82 dB. The performance was attributed to the "synergistic effects and interfacial polarization between Fe₃O₄ nanoparticles and graphite". The composite materials have electromagnetic absorption peaks in both the C-band and Ku-band, therefore with relevance for 5G technology and the shielding absorption of C-band radar waves (Wang et al., 2022).

Here the point of view by Wang and coworkers about Fe₃O₄ nanoparticles. "Among various electromagnetic microwave absorption materials", these nanoparticles have the advantages of being environmental friendly material, abundant, and with controllable preparation technology. Wang et al. provide several references to research studies about composites of Fe₃O₄ with carbon-based materials (see references in Wang et al., 2022). For what regards graphite, it "is one of the early aircraft skin inter-layer-filled absorbing materials. Due to the stacked structure of graphite sheets, it has specific absorbing properties" (Wang et al., 2022, Peng, et al., 2018). Graphite has a low density, accompanied by a high specific surface area, with good electrical conductivity. Combined with Fe₃O₄ nanoparticles, the material is a composite which both magnetic loss and electrical loss, with improved impedance matching characteristics. "Finally, the reflection loss of Fe₃O₄ generally occurs at a lower frequency region, and the reflection loss of graphite is usually located in the high-frequency region" (Wang et al., 2022). In this manner, the interval of absorption is expanded.

"The magnetic loss of materials mainly comes from the domain wall resonance, eddy current effect, hysteresis loss, natural resonance, and exchange resonance" (Wang et al., 2022), but in the case of Fe₃O₄, domain wall resonance and hysteresis losses are not the principal mechanism of magnetic loss in Fe₃O₄–PG. The magnetic loss is dominated by natural resonance in the range of 2–10 GHz, and by eddy current loss in the range of 10–18 GHz.

### Nanoparticles and textiles

Let us return to textile applications and ICPs. Saini et al., 2012, proposed composites using polyaniline-coated cotton fabrics, incorporating in the coating some dielectric and magnetic nanoparticles (BaTiO₃ and Fe₃O₄ nanoparticles into polyaniline, PANI, matrix). The researchers used a surfactant, the dodecylbenzenesulfonate (DBSA), to have a uniform dispersion of inorganic fillers, BaTiO₃ or Fe₃O₄. As discussed by Saini et al., the uniform dispersion of nanoparticles within the polymer is fundamental. The researchers observed that, with a relatively high density of ferrites and/or titanate fillers, a poor dispersion of these fillers in the polymer can be observed. The poor dispersion produces a phase separation and a consequent heterogeneity which is deteriorating the properties of the composite with respect the electromagnetic shielding (Saini et al., 2012). The aqueous solutions of amphiphilic molecules, in this case of DBSA, due to its viscosity, is able of avoiding the agglomeration of the fillers (Saini et al., 2012). Dielectric measurements give that the incorporation of BaTiO₃ is increasing the dielectric properties of PANI, the same from magnetization measurements that show the relevance of the incorporation of Fe₃O₄ in the improvement of magnetic properties. Saini and coworkers obtained specific shielding effectiveness value of 17–20 dB cm³/g, indicating accordingly that the composite fabric can be used for microwave-shielding application.

Recently, Yörük et al., 2021, deposited PANI with nanoparticles onto polypropylene PP nonwoven, so that this relevant nonwoven could be used to create an EMI shield. The magnetic nanoparticles used by the researchers were Fe₃O₄, CoFe₂O₄, and MnFe₂O₄. We find again double-coated materials. The composite based on PP, MnFe₂O₄, and polyaniline displayed the highest attenuation (94.2% at 2.11 GHz), dominated by absorption, with 12.4 dB EMI-SE (Yörük et al., 2021).

Hollow magnetic Fe₃O₄ nanospheres have been also used for flexible nonwoven fabrics, by Zheng et al., 2023. The Fe₃O₄/MXene, that is a transition metal carbide, composite fabric has an EMI-SE of 33.28 dB. The EMI shielding mechanism is "tunable" thanks to the loaded materials. In this manner, as interestingly stressed by the researchers, "the mechanism can alternate from absorption to reflection" (Zheng et al.,

2023). To have a lighter weight, the nanoparticles are hollow, a strategy already pursued in the past.

**Fe₃O₄/CarbonBlack@Epoxy-Resin-Matrices**
Fallah et al., 2022, studied the EMI shielding properties of polymer nanocomposites possessing different weight percentages of Fe₃O₄ nanoparticles and of "cost-effective" carbon black nanoparticles (CBNs). Nanocomposites were prepared by mixing and casting. EMI-SE was investigated in the frequency range of 8.2 ~ 12.4 GHz. The maximum SE was 36.6 dB at 8.2 GHz for a composite with weight percentage of 15% Fe₃O₄ and 50% CBN (0.7 mm thickness).

About composites, it is told that an epoxy resin (EI-403, Mokarrar Engineering Material Co. Nanomaterials) was the matrix, spherical nanoparticles CBN and Fe₃O₄ were the fillers. Fallah and coworkers tell that "the high electrical conductivity of Fe₃O₄ and CBN is one of the main reasons" for the high EMI-SE observed for their composites. However, "the distribution of CBN is also significant. The uniform distribution of Fe₃O₄ and CBN particles in the matrix established a conducting network", which is increasing EMI-SE (Fallah et al., 2022). Moreover, "the proper combination of electrical and magnetic losses causes excellent wave absorption" (Fallah et al., 2022).

**Film depositions**
The nanoparticles have been discussed at length; however, we have at the beginning mentioned the case of polypyrrole and magnetite composite films, developed by Yan et al., 2001. An electrode, covered with PPy film, was used for the electrodeposition of magnetite film. On this film, used as a working electrode, polypyrrole was deposited again. A final PPy/Fe₃O₄/PPy "sandwich" composite film was obtained. Yan et al. are not discussing the microwave absorption of the sandwich. However, microwave transmission, reflection, and absorption behavior of films of electrochemically synthesized polypyrrole has been given by Kaynak et al., 1994. As determined by Kaynak and coworkers, the electrical conductivity of doped polypyrrole films has a significant role regarding transmission, reflection, and absorption of microwaves. When the film is heavily doped, it is highly reflective. If it is lightly doped, the film has high transmission. Intermediate doping of polypyrrole produces films which are highly absorptive.

Returning to magnetic films, we can see that, in a quite different form, the electromagnetic and microwave absorption properties have been investigated. Wei et al., 2007, used Fe₃O₄ magnetic films plated on hollow glass spheres, to obtain spheres–wax composites. Wei and coworkers observed an improvement of dielectric and magnetic losses, as the volume fraction of the magnetic spheres in the composites increased. The researchers concluded that microwave absorption was

mainly coming from the magnetic loss (Wei et al., 2007). Fe₃O₄ films on hollow spheres or other low-density materials is a good solution to substitute the conventional absorbing materials, ferrites for instance, which have good absorbing properties but are too heavy. To solve the same problem, Qiang et al., 2010, used carbon fibers as a substrate with low density but high strength, and good electrical properties. Therefore, the "composites of carbon fibers and magnetic materials" have a lighter weight accompanied by good conductivity and strength. As stressed by Qiang and coworkers, Fe₃O₄ is exhibiting "excellent microwave absorption property", and can be used in several applications.

Li et al., 2013, proposed electroless Ni-Fe₃O₄ composite plating on polyester fabric modified with 3-aminopropyltrimethoxysilane. The EMI-SE of Ni-Fe₃O₄ plated polyester fabric were evaluated. With a Ni-Fe₃O₄ weight on the treated fabric of 32.90 g/m², the EMI SE arrives to 15–20 dB for frequencies in the range from 8 to 18 GHz. The results indicate an EMI shielding use of the material (Li et al., 2013).

**Paramagnetism and magnetocaloric effect**
According to Wei et al., 2012, Fe₃O₄ nanoparticles have been intensively investigated because of their super-paramagnetic behavior and for their low Curie temperature. The nanoparticles are also non-toxic and biocompatible, and therefore have several biomedical applications. In the super-paramagnetism, and in the absence of an external magnetic field, the magnetization appears to be zero, when averaged on a time longer than Néel relaxation time. If an external magnetic field is applied, nanoparticles behave as paramagnets, with a magnetic susceptibility which is larger than that of paramagnets. Linked to the paramagnetism, we find the magnetocaloric effect. This effect is the adiabatic temperature change of a material upon application of a magnetic field (McMichael et al., 1991).

"By grouping spins together in superparamagnetic clusters", McMichael and coworkers explain, magnetic moments are easily aligned in paramagnetic systems. "For certain ranges of field, temperature and cluster size, the entropy of the spins is more easily changed by application of a field" (McMichael et al., 1991). Magnetocaloric effect is therefore a heating or cooling of a material due to the coupling between the magnetic moments and external magnetic field. In the following Section, we will find that the magnetocaloric effect has been involved in new materials based on biochar.

**Black magnetic biochar**
Biochar is the black fine-grained residue of the pyrolysis of biomass. It is the product of a thermochemical decomposition at moderate temperatures under oxygen-limiting conditions. This

residue has a pore structure with large specific surface area, due to the presence of a mesoporous framework in it. For this reason, biochar can be used for producing shape-stabilized phase change materials SSPCMs (Sparavigna, 2022). The biochar mesoporous framework can encapsulate the liquid phase of PCMs, that are substances absorbing and releasing thermal energy at phase transitions, overcoming the leakage problem of them. One of these SSPCMs is a "black magnetic biochar".

Biochar has several applications. Its main use is for soil emendation, but it can also be used as a filler in polymers and concrete (Brassard et al., 2019, Ok et al., 2015, Bartoli et al., 2020, Ziegler et al., 2020), even for electromagnetic shielding (see Appendix). In the recent review by Liang et al., 2022, about phase-change materials, a section of the article is devoted to the use of biochar-based composite PCMs for the storage of solar energy, in the form of thermal energy. Among the reported literature, we can find the article by Yang et al., 2019. The researchers used poplar wood powder to obtain carbonized wood powder (CWF), and then synthesized CWF-PCMs. $Fe_3O_4$ nanoparticles have been introduced to prepare a composite able to improve the solar thermal efficiency of CWF-PCMs, because the $Fe_3O_4$ nanoparticles are adding - as told by Liang et al. - a "black appearance" to biochar so that the absorbed sunlight is increased.

Yang et al., 2019, stress that the composite is a "magnetic wood-based composite phase change material". The researchers used $Fe_3O_4$ nanoparticles and melted 1-tetradecanol mixed together in weight ratios of 1:100, 2:100, 5:100, and 8:100. The $Fe_3O_4$ nanoparticles provide magnetic property to the composite. Due to the magnetothermal effect, the composite "can be heated under an alternating magnetic field". The magnetic wood-based composite PCM has a latent heat as large as 179 J/g.

Yang and coworkers do not investigate the properties of the composite related to EMI shielding. This has been made by Shen et al., 2022, who have produced biomass-based carbon aerogels, used as porous supporting material to encapsulate magnetic $Fe_3O_4$@polyethylene glycol by vacuum impregnation. The researchers say that they have obtained "excellent thermal storage capability and satisfactory EMI shielding effectiveness (SE)". "With addition of 7 wt% $Fe_3O_4$," one of the PCMs achieves EMI SE of 53.83 dB. (Shen et al., 2022).

Lignin and graphene oxide (GO) are used by Yang et al.; GO has good mechanical behavior and the electrical conductivity. The lignin@GO suspensions were obtained using several ratios of lignin and GO by stirring and sonication. The lignin@GO suspensions were freeze-dried and thermal annealed to have LG aerogels. Then, LGs were impregnated by pure PEG

under vacuum LGs were also impregnated in Fe3O4@PEG with different mass ratios of $Fe_3O_4$.

Of course, we could also use the $Fe_3O_4$@PPy core/shell nanoparticles, those proposed by Li et al., 2011, or those by Deng et al., 2003, in the paraffin wax and stabilize them in the macropores of biochar.

For what is regarding the EMI SE performance of biochar composites, the recent article by Nikolopoulos et al., 2023, stresses that the biochar-based composites "are multi-functional materials with a wide range of environmental and other applications. A new and emerging application is … as materials with significant electromagnetic shielding effectiveness". Nikolopoulos and coworkers used olive tree pruning biochar for composite samples with carbon black and polytetrafluoroethylene as binder. "Modifying biochar with the 20 %w/w acetylene black largely increased its shielding effectiveness, reaching the value of 39 dB" (Nikolopoulos, 2023).

**Biochar and other microwave absorption materials**
An interesting approach is that proposed by Chen et al., 2023. The researchers are disclosing a facile fabrication of biochar absorbers for enhanced microwave absorption, based on $Fe_3O_4$ nanoparticles. According to the researchers, the "biochar microwave absorption (MA) materials are attracting significant attention due to their sustainability and cost-effective features". However, to have a significant MA performance, it is necessary to load the biochar with magnetic nanoparticles (NPs). The used approach is based on biotemplates, with Spirulina (SP) cells loaded with $Fe_3O_4$ NPs.

This biochar is not alone, and Chen and coworkers are reporting several studies on biochar absorbers, which "have gained particular attention due to their unique advantages, including porous structures, superior dielectric loss, low cost, and robust properties" (Zhao et al., 2019, Guan et al., 2021, Natalio et al., 2020). EMI-SE is based on the major mechanisms of reflection, multireflection and absorption. For electromagnetic absorption, as we have previously seen, it is required the "synergistic effect" between electric and magnetic dipoles. Carbon-based materials loaded with metal oxide nanoparticles possessing a high dielectric constant, have been investigated for EMI absorption, but - as stressed by Chen et al. - to improve the magnetic loss of absorbers, the loading of magnetic nanoparticles "not only optimize the impedance matching, but also enhance the overall MA [microwave absorption] performances via synergistic effects of both magnetic and dielectric losses". And therefore we can find the biochar composites (Jute/$Fe_3O_4$, Coconut shell/FeOx, Pine nut shell/NiO, Glucose/$Fe_3O_4$, Rice husk/Co, Eggplant peal/Ni), fabricated as biochar absorbers with loading of

magnetic NPs (Fang et al., 2017, Liu et al., 2019, Wang et al., 2019, Wang et al., 2022).

Yin et al, 2021, prepared cotton-derived carbon fibers and hollow $Fe_3O_4$/CoFe hybrids via a two-stage method of hydrothermal and calcination. These hybrids are defined by Yin and coworkers as *biochar* and are proposed as novel low-frequency microwave absorbers. Because of the combined effect of magnetic and dielectric losses, the ternary hybrid possesses "outstanding low-frequency microwave absorbing capacity". The maximal reflection loss values can reach about 40.15 dB. Yin and coworkers claim that the biochar "exhibits huge potential in electromagnetic absorption owing to its rich structures, *splendid* performance, light weight, extensive source, pro-environment and low cost". Pengfei Yin and coworkers had also reported in 2020 the "reclaimed straw of sorghum derived biochar/(Fe,Ni) hybrid", prepared via a facile calcination process, as possessing "an outstanding low-frequency electromagnetic absorbing performance. Besides sorghum, ammonium hydroxide, ethanol, ferric nitrate nonahydrate and nickel nitrate have been used too.

Among the references given by Yin et al., 2021, we find literature where "biochar-based MAMs present *wonderful* microwave absorbing performance in relatively high-frequency range," so that practicability of biochar for microwave absorption is indicated (Yin et al., 2021). Lou et al., 2018, are displaying the synthesis of magnetic wood fiber boards with electromagnetic wave absorbing properties. In Lv et al., 2016, the article is proposing bacterial cellulose functionalized by sputtering with copper (Cu) and $Al_2O_3$ to endow it with EMI shielding properties (EMI-SE 65.3 dB). Marins et al., 2013, are proposing flexible magnetic membranes "with high proportion of magnetite", prepared by impregnation of bacterial cellulose pellicles with ferric chloride, then followed "by reduction with sodium bisulfite and alkaline treatment for magnetite precipitation" (Marins et al., 2013). Microwave properties of the pellicles were investigated in the X-band (8.2 to 12.4 GHz), and the researchers concluded "a potential application as microwave absorber materials" (Marins et al., 2013).
Other reference given by Yin et al, 2021, are reporting a variety of biomass-based carbon materials being "hierarchically porous carbons (HPCs) with excellent

microwave absorption (MA) performance" (Wu et al., 2018), with "embedded alkaline metal elements" which are those inside the materials from which biochar is derived. Carbon foams, with "excellent electromagnetic wave absorption performance", are mentioned too (Zhou et al., 2019).

Yin et al, 2021, are also referring to the work by Wang et al., 2018. Materials are based on loofah sponge as hierarchical porous carbon precursors and ferric nitrate as magnetic precursor. The carbonization process turns the structure of loofah sponge into "interconnected networks with hierarchical porous structures, and the precursor ferric nitrate converts into magnetic $Fe_3O_4$@Fe nanoparticles" (Wang et al., 2018). The resulting porous carbon/$Fe_3O_4$@Fe composites "exhibit outstanding MA performance" (Wang et al., 2018). Wang and coworkers are giving minimum reflection loss (RL) of −49.6 dB with a thickness of 2 mm.

To the above-mentioned works let us add Pan et al., 2022, who are proposing a wood-based composite, consisting in a multilayer structure having a positive conductance gradient and negative magnetic gradient, so that the electromagnetic waves are trapped to underwent a sequence of absorption, reflection and reabsorption, with an additional interfacial polarization loss-induced absorption process. The electromagnetic shielding of the composite can be up to 94.73 dB ranging from 300 kHz to 3.0 GHz.

Since we are talking about wood, let us consider that its lignin is also involved in EMI shielding by Hu et al., 2021. Hu and coworkers prepared "flexible lignin-based electromagnetic shielding polyurethane (FeCLPU) with *excellent* properties". Lignin was used with carbon nanotubes (CNTs) and $Fe_3O_4$ nanoparticles in polyurethane "to improve electromagnetic shielding properties" (Hu et al., 2021). The KH550 coupling agent was used for $Fe_3O_4$. The modified nanoparticles were mixed with lignin, polyethylene glycol (PEG), hexamethylene diisocyanate (HDI) and CNTs to synthesize FeCLPU. "When the concentrations of both $Fe_3O_4$ and CNT were 10% and the lignin content was 15%, the maximum EMI SE reached 37.5 dB" (Hu et al., 2021).
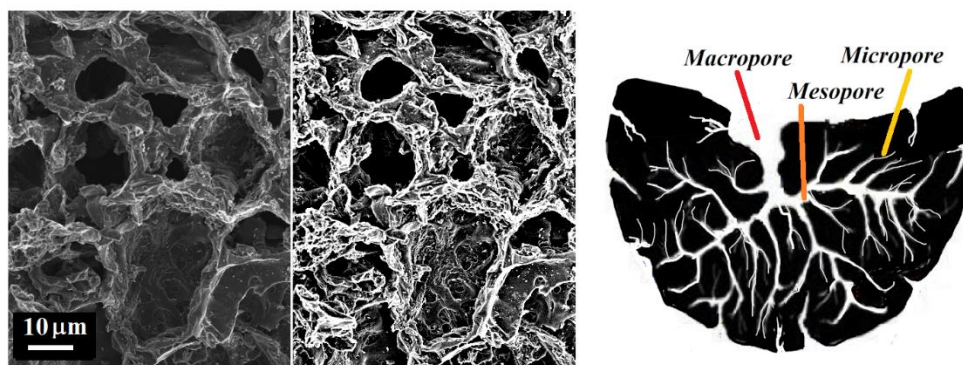
–Fig. 6: On the left and middle, a detail of a scanning electron microscope image of biochar from ground coffee (image courtesy Mauro Giorcelli, Department of Applied Science and Technology, Polytechnic University of Turin, Italy; discussion about coffee biochar is given in Giorcelli and Bartoli, 2019). On the right, the hierarchy of the pores in biochar. We can see the pores from macro- to micro size. Let us note that the cavities which we can see in the SEM imagery, as in the left image, are much larger than the macropores sketched on the right. According to IUPAC classification, micropores have size less than 2 nm, mesopores from 2 nm to 50 nm, and macropores have size greater than 50 nm. Then, we must imagine the walls of the cavities shown by the SEM imagery pierced by the apertures of macropores. From macropores the mesopores are departing to reach the micropores. Some very large macropore apertures on the biochar cavity walls seem being visible in the same SEM image, courtesy M. Giorcelli.
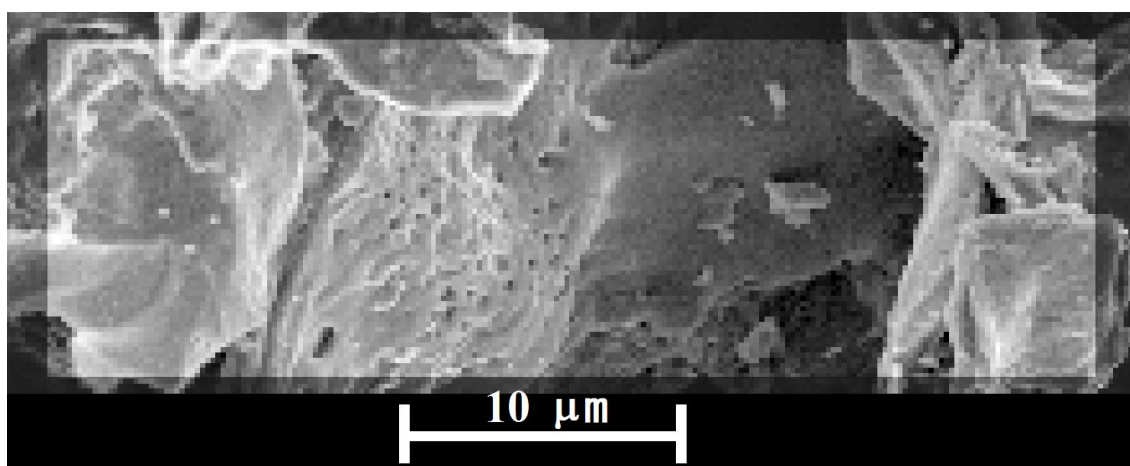


Fig. 7 : A detail (processed to enhance luminosity and contrast) of the SEM image of biochar, Fig.6, from ground coffee (image courtesy Mauro Giorcelli, Polytechnic University of Turin, Ref. Giorcelli & Bartoli, 2019). As previously told, we must imagine the walls of biochar cavities pierced by the relatively large apertures of macropores.

### Fe₃O₄@Honeycomb

Gao et al., 2018, considered honeycomb-like carbonaceous composites to enhance the performance of Fe₃O₄ based absorbing materials. Carbon nanotubes, filaments, fibers, and chemically derived graphene, considered for electromagnetic wave absorbers, "have many disadvantages", and Gao and coworkers mentioned them. For instance, carbon nanotubes and graphene can undergo "restacking and aggregation during the preparation process" (Gao et al., 2018), and this fact could influence negatively the final properties of the material. Moreover, the cost of materials and processing is rather relevant. A carbonaceous material, the biochar, exists which is otherwise largely applied (Gao et al., 2018). Gao and coworkers are mentioning that biochar possesses intrinsic porosity, with large specific surface areas and oxygen-containing functional groups. Moreover, biochar can be activated with KOH so that a considerable number of mesopores is formed inside

the material. If biochar were used to produce microwave absorber composites, the energy of the microwaves "would be effectively attenuated by interfacial polarization relaxation loss", because of the solid–void interfaces (Gao et al., 2018). And here we can find again what we have previously told when mentioning Qin et al., 2022. The activation with KOH is increasing mesoporosity and consequently the loss due to interface polarization.

Gao and coworkers are mentioning the work by Qiu et al., 2017, who used walnut shell-derived nano-porous carbon to produce a microwave absorber based on dielectric loss, but the magnetic loss mechanism was not involved. The researchers considered the use of Fe₃O₄ nanoparticles because of their chemical and thermal stability and proper magnetization features. They prepared a honeycomb-like carbonaceous composite, with a tailored porous framework with Fe₃O₄ NPs. The framework was obtained from walnut

shells too. These shells were subjected to two carbonization processes, one at 400 °C, the second at 600 °C after etching with KOH. Then, the porous carbonaceous framework was decorated with $Fe_3O_4$ nanoparticles. The microwave analysis, - and let us stress once more this fact - shows a "synergistic effect between the porous architectures and magnetic species" (Gao et al., 2018). Gao and coworkers measured the complex permittivity and permeability of the composite, showing that the decoration of the honeycomb by means of magnetite NPs, is increasing the $\varepsilon'$ values of the composite. The higher $\varepsilon'$ values can come from space charge polarization caused by the heterogeneity of composite (Gao et al., 2018). The decoration of the surface of porous carbon with nanoparticles generates more space charge and accumulation at the interface, and this contributes to higher microwave absorption in the composite. Let us stress once more that the KOH etching improved the microwave absorption because of an increase in the dielectric loss due to the induced numerous defects and mesoporosity (Gao et al., 2018).

Let us add that walnut shells have been used also by Li et al., 2020, decorated by $Fe_3O_4$. And Jia et al., 2021, used $Fe_3O_4/\alpha$-Fe decorated porous carbon-based composites to adjust impedance matching.

**Preparing Fe₃O₄@Biochar**
We have found that, in the case of the biochar as shape-stabilizer material for PCMs, $Fe_3O_4$ nanoparticles have been inserted in the fluid PCM then impregnated in biochar. However, according to the previously proposed literature, the main approach for EMI shielding seems being that of using precursors for the creation of magnetic nanoparticles. Here, let us also propose the method we find in Li et al., 2016, to have $Fe_3O_4$@Biochar. The spongy pomelo pericarp is used for biochar, grounded into fine powders. Biochar of 1.0 g is mixed with 5.22 g $Fe(NO_3)_3\cdot9H_2O$ (that is, ferric nitrate, iron nitrate, Iron(III) nitrate nonahydrate) in 50 mL water. After 1 hour of intense stirring, the mixture is desiccated and dried for 12 hours. Then, it is put into a tube furnace and heated in flowing $N_2$, and the product is denoted as $Fe_3O_4$ NP/C (see all details in the article by Li et al., 2016). In the case the as-prepared biochar of 1.0 g is soaked with 1 M nitric acid, the acid-treated carbon (AC) is composited to have $Fe_3O_4$ NP/AC. In the $Fe_3O_4$@Biochar, "the mineral substances of uniformly distributed KCl and $CaCO_3$ in the biochar play an important role in enhancing the electrochemical performance of the composite", so that Li et al., 2016, are proposing this composite for anode materials for Li-ion batteries. This composite can have EMI shielding properties too, and could be interestingly processed to have synergistic effects among the porous structure of biochar and the losses produced by dielectric and magnetic nanoparticles (Gao et al., 2018). Actually, several $Fe_3O_4$@biochar composites

exist which are used in applications different from EMI shielding. They could be interestingly investigated for the microwave absorption.

**A review**
As in many other cases, today we are facing a strong increase of the number of publications about new composite materials. This is true also for composites based on the magnetite nanoparticles that we have here discussed. Searching by means of Scholar - fe3o4 nanoparticles electromagnetic shielding - about 21,000 results are proposed. Then, the references here given could appear as "rari nantes in gurgite vasto" (Virgil, Aeneid, I, 188), sparse elements in the immense sea. To navigate this sea, the compass was that of considering the beneficial effect that $Fe_3O_4$ nanoparticles can have on some materials, such as ICPs, which are already interesting for EMI shielding by themselves.

We have also proposed the new composites based on biochar. Biochar is remarkable for its hierarchical porous structure, so that bare or core/shell nanoparticles can be easily inserted in its macropores, enhancing biochar intrinsic EMI shielding features.

The proposed review could be expanded to more cases, but there is a key obstacle which is hampering any discussion about EMI shielding in composite materials. It is the fact that experimental results are proposed in rather different manners, sometimes turning them into data which are difficult to compare. We have shielding effectiveness SE and reflection loss RL to evaluate and compare.

Wang et al., 2011, have clearly told the reason for investigating RL of materials, which is that of finding "a dip in reflection loss (RL) in the desired frequency range". Researchers have also remarked that, away from what we need, "even an excellent microwave absorbing capability seems useless" (Wang et al., 2011). Consequently, a large part of the literature here proposed is based on the "quarter-wavelength model" (the single-layered plane wave absorber backed by a perfect conductor). This model seems to be today the standard model for materials scientists. However, for application the EMI-SE shielding effectiveness is relevant too.

**Appendix: biochar@concrete**
About biochar, we have mentioned the fact that it is compatible with concrete. A recent review about the use of biochar in concrete (Singhal, 2022), tells that biochar is an efficient absorber for EM radiations, besides allowing "buildings to be turned into carbon sinks". Singhal mentions the works by Yasir et al., 2020, who studied shielding properties of cement composites with commercial biochar. At 10 GHz, SE of plain cement was almost 5 dB; for samples with 14 wt.% biochar, SE was of 11 dB, and of 15 dB with 18

wt.% (4-mm-thick samples) (Yasir et al., 2020). Savi et al. (2020) used biochar derived from sewage sludge obtaining SE around 10 dB in the presence of 20% biochar (Savi et al., 2020).

Since our discussion is about the role of magnetite in electromagnetic shielding, let us consider the work by Das et al., 2022. The study focused on developing EMI shielding cement-based concrete; a maximum SE - around three times than of normal concrete with a similar range of compressive strength - was achieved in conductive concrete with magnetite and graphite aggregates and 2% steel fibres.

For what is regarding the use of biochar in different matrices (included concrete) for EMI-SE evaluation, see please Torsello et al., 2021. Torsello and

coworkers reported microwave shielding efficiency in the frequency range 100 MHz–8 GHz. Samples have thickness of 10 and 30 mm. In case of biochar as a filler, as told by Torsello and coworkers, "several aspects intervene due to its intrinsically disordered nature and to the large range of graphitization degrees that can be obtained" in preparing the material; however, "the main contributions to EM shielding in such materials are expected to stem from migration and hopping conductance" (Torsello et al. mentioning Cao et al., 2010). For data comparison, we invite the reader to consider the already mentioned article by Nikolopoulos et al., 2023, which is giving a characterization of the EMI SE of biochar and biochar-based materials.

## References

1. Adebayo, L. L., Soleimani, H., Yahya, N., Abbas, Z., Wahaab, F. A., Ayinla, R. T., & Ali, H. (2020). Recent advances in the development OF Fe3O4-BASED microwave absorbing materials. Ceramics International, 46(2), 1249-1268.
2. Arora, M., Wahab, M. A., & Saini, P. (2014). Permittivity and electromagnetic interference shielding investigations of activated charcoal loaded acrylic coating compositions. Journal of Polymers, 2014.
3. Avloni, J., Florio, L., Henn, A. R., Lau, R., Ouyang, M., & Sparavigna, A. (2006). Electromagnetic shielding with polypyrrole-coated fabrics. arXiv preprint cond-mat/0608664.
4. Avloni, J., Ouyang, M., Florio, L., Henn, A. R., & Sparavigna, A. (2007). Shielding effectiveness evaluation of metallized and polypyrrole-coated fabrics. Journal of Thermoplastic Composite Materials, 20(3), 241-254.
5. Avloni, J., Lau, R., Ouyang, M., Florio, L., Henn, A. R., & Sparavigna, A. (2008). Polypyrrole-coated nonwovens for electromagnetic shielding. Journal of Industrial Textiles, 38(1), 55-68.
6. Bartoli, M., Giorcelli, M., Jagdale, P., Rovere, M., & Tagliaferro, A. (2020). A review of nonsoil biochar applications. Materials, 13(2), 261.
7. Blaney, L. (2007). Magnetite (Fe3O4): Properties, synthesis, and applications. Lehigh Preserve Collection, Volume 15, Paper 5. http://preserve.lehigh.edu/cas-lehighreview-vol-15/5
8. Brassard, P., Godbout, S., Lévesque, V., Palacios, J. H., Raghavan, V., Ahmed, A., Hogue, R., Jeanne, T., & Verma, M. (2019). Biochar for soil amendment. In Char and carbon materials derived from biomass (pp. 109-146), Elsevier, 2019.
9. Brodie, G., Jacob, M. V., & Farrell, P. (2015). Microwave and radio-frequency technologies in agriculture. In Microwave and Radio-Frequency Technologies in Agriculture. De Gruyter Open Poland.
10. Cao, M.S., Song, W.L., Hou, Z.L., Wen, B., & Yuan, J. (2010). The effects of temperature and frequency on the dielectric properties, electromagnetic interference shielding and microwave-absorption of short carbon fiber/silica composites. Carbon, 48, 788–796.
11. Cao, M.S., Yang, J., Song, W.L., Zhang, D.Q., Wen, B., Jin, H.B., Hou, Z.L., & Yuan, J. (2012). Ferroferric oxide/multiwalled carbon nanotube vs polyaniline/ferroferric oxide/multiwalled carbon nanotube multiheterostructures for highly effective microwave absorption. ACS applied materials & interfaces, 4(12), 6949-6956.
12. Chakradhary, V. K., Juneja, S., & Akhtar, M. J. (2020). Correlation between EMI shielding and reflection loss mechanism for carbon nanofiber/epoxy nanocomposite. Materials Today Communications, 25, 101386.
13. Chen, X., Gu, Y., Liang, J., Bai, M., Wang, S., Li, M., & Zhang, Z. (2020). Enhanced microwave shielding effectiveness and suppressed reflection of chopped carbon fiber felt by electrostatic flocking of carbon fiber. Composites Part A: Applied Science and Manufacturing, 139, 106099.
14. Chen, T., Cai, J., Gong, D., Liu, C., Liu, P., Cheng, X., & Zhang, D. (2023). Facile fabrication of 3D biochar absorbers dual-loaded with Fe3O4 nanoparticles for enhanced microwave absorption. Journal of Alloys and Compounds, 935, 168085.
15. Cornell, R. M., & Schwertmann, U. (1996). The iron oxides. VCH Press, Weinheim, Germany.
16. Das, N., Mahadela, A. S., Nanthagopalan, P., & Verma, G. (2022). Investigation on electromagnetic pulse shielding of conductive concrete. Proceedings of the Institution of Civil Engineers-Construction Materials, 1-16.
17. Deng, J., Peng, Y., He, C., Long, X., Li, P., & Chan, A. S. (2003). Magnetic and conducting Fe3O4–polypyrrole nanoparticles with core-shell structure. Polymer international, 52(7), 1182-1187.
18. Deng, L., & Han, M. (2007). Microwave absorbing performances of multiwalled carbon nanotube composites with negative permeability. Applied physics letters, 91(2), 023119.
19. Dey, A., De, A., & De, S. K. (2005). Electrical transport and dielectric relaxation in Fe3O4–polypyrrole hybrid nanocomposites. Journal of Physics: Condensed Matter, 17(37), 5895.
20. Ding, J., Wang, L., Zhao, Y., Xing, L., Yu, X., Chen, G., Zhang, J., & Che, R. (2019). Boosted interfacial polarization from multishell TiO2@ Fe3O4@ PPy heterojunction for enhanced microwave absorption. Small, 15(36), p.1902885.
21. Du, Y., Liu, W., Qiang, R., Wang, Y., Han, X., Ma, J., & Xu, P. (2014). Shell thickness-dependent microwave absorption of core–shell Fe3O4@C composites. ACS applied materials & interfaces, 6(15), 12997-13006.
22. Everaere, E. (2015). Polarimetry in bistatic configuration for ultra high frequency radar measurements on forest environment (Doctoral dissertation, Ecole Polytechnique).
23. Fallah, R., Hosseinabadi, S., & Pourtaghi, G. (2022). Influence of Fe3O4 and carbon black on the enhanced electromagnetic interference (EMI) shielding effectiveness in the epoxy resin matrix. Journal of Environmental Health Science and Engineering, 20(1), 113-122.
24. Fang, J., Shang, Y., Chen, Z., Wei, W., Hu, Y., Yue, X., & Jiang, Z. (2017). Rice husk-based hierarchically porous carbon and magnetic particles composites for highly efficient electromagnetic wave attenuation. Journal of Materials Chemistry C, 5(19), 4695-4705.
25. Ganguly, S., Bhawal, P., Ravindren, R., & Das, N. C. (2018). Polymer nanocomposites for electromagnetic interference shielding: a review. Journal of Nanoscience and Nanotechnology, 18(11), 7641-7669.
26. Gao, S., An, Q., Xiao, Z., Zhai, S., & Shi, Z. (2018). Significant promotion of porous architecture and magnetic

Fe3O4 NPs inside honeycomb-like carbonaceous composites for enhanced microwave absorption. RSC advances, 8(34), 19011-19023.

27. Giorcelli, M., & Bartoli, M. (2019). Development of coffee biochar filler for the production of electrical conductive reinforced plastic. Polymers, 11(12), 1916.

28. Guan, H., Wang, Q., Wu, X., Pang, J., Jiang, Z., Chen, G., Dong, C., Wang, L., & Gong, C. (2021). Biomass derived porous carbon (BPC) and their composites as lightweight and efficient microwave absorption materials. Composites Part B: Engineering, 207, p.108562.

29. Guo, J., Song, H., Liu, H., Luo, C., Ren, Y., Ding, T., Khan, M.A., Young, D.P., Liu, X., Zhang, X. and Kong, J., 2017. Polypyrrole-interface-functionalized nano-magnetite epoxy nanocomposites as electromagnetic wave absorbers with enhanced flame retardancy. Journal of Materials Chemistry C, 5(22), pp.5334-5344.

30. Katsenelenbaum, B. Z. (2006). High-frequency electrodynamics. John Wiley & Sons.

31. Kaynak, A., Unsworth, J., Clout, R., Mohan, A. S., & Beard, G. E. (1994). A study of microwave transmission, reflection, absorption, and shielding effectiveness of conducting polypyrrole films. Journal of applied polymer science, 54(3), 269-278.

32. Kruželák, J., Kvasničáková, A., Hložeková, K., Plavec, R., Dosoudil, R., Gořalík, M., Vilčáková, J. , & Hudec, I. (2021). Mechanical, Thermal, Electrical Characteristics and EMI Absorption Shielding Effectiveness of Rubber Composites Based on Ferrite and Carbon Fillers. Polymers, 13(17), 2937.

33. Henn, A.R., & Silverman, B. (1991). New Developments in Metallized Products, Interference Technology Engineering Master (ITEM) Update, pp. 180-187.

34. Henn, A. R., & Cribb, R. M. (1993). Modelling the shielding effectiveness of metallized fabrics, Interference Technology Engineering Master (ITEM) Update, p. 49-57.

35. Hosseini, S. H., Mohseni, S. H., Asadnia, A., & Kerdari, H. (2011). Synthesis and microwave absorbing properties of polyaniline/MnFe2O4 nanocomposite. Journal of Alloys and Compounds, 509(14), 4682-4687.

36. Hu, W., Zhang, J., Liu, B., Zhang, C., Zhao, Q., Sun, Z., Cao, H., & Zhu, G. (2021). Synergism between lignin, functionalized carbon nanotubes and Fe3O4 nanoparticles for electromagnetic shielding effectiveness of tough lignin-based polyurethane. Composites Communications, 24, p.100616.

37. Jia, C., Xia, T., Ma, Y., He, N., Yu, Z., Lou, Z., & Li, Y. (2021). Fe3O4/α-Fe decorated porous carbon-based composites with adjustable electromagnetic wave absorption: impedance matching and loading rate. Journal of Alloys and Compounds, 858, 157706.

38. Katsenelenbaum, B. Z. (2006). High-frequency electrodynamics. John Wiley & Sons.

39. Kruželák, J., Kvasničáková, A., Hložeková, K., Plavec, R., Dosoudil, R., Gořalík, M., Vilčáková, J. and Hudec, I., 2021. Mechanical, Thermal, Electrical Characteristics and EMI Absorption Shielding Effectiveness of Rubber Composites Based on Ferrite and Carbon Fillers. Polymers, 13(17), p.2937.

40. Le Bolay, N., Lakhal, R., & Hemati, M. (2020). Production of Hematite Micro-and Nanoparticles in a Fluidized Bed Process—Mechanism Study. KONA Powder and Particle Journal, 37, 244-257.

41. Lee, Y., Lee, J., Bae, C. J., Park, J. G., Noh, H. J., Park, J. H., & Hyeon, T. (2005). Large-scale synthesis of uniform and crystalline magnetite nanoparticles using reverse micelles as nanoreactors under reflux conditions. Adv. Funct. Mater. 15, 503-509

42. Li, Y., Chen, G., Li, Q., Qiu, G., & Liu, X. (2011). Facile synthesis, magnetic and microwave absorption properties of Fe3O4/polypyrrole core/shell nanocomposite. Journal of Alloys and Compounds, 509(10), 4104-4107.

43. Li, Y., Lan, J., Guo, R., Huang, M., Shi, K., & Shang, D. (2013). Microstructure and properties of Ni-Fe3O4 composite plated polyester fabric. Fibers and Polymers, 14(10), 1657-1662.

44. Li, T., Bai, X., Qi, Y. X., Lun, N., & Bai, Y. J. (2016). Fe3O4 nanoparticles decorated on the biochar derived from pomelo

pericarp as excellent anode materials for Li-ion batteries. Electrochimica Acta, 222, 1562-1568.

45. Li, D., Liang, X., Quan, B., Cheng, Y., Ji, G., & Du, Y. (2017). Investigating the synergistic impedance match and attenuation effect of Co@ C composite through adjusting the permittivity and permeability. Materials Research Express, 4(3), 035604.

46. Li, Z., Lin, H., Ding, S., Ling, H., Wang, T., Miao, Z., Zhang, M., Meng, A., & Li, Q. (2020). Synthesis and enhanced electromagnetic wave absorption performances of Fe3O4@C decorated walnut shell-derived porous carbon. Carbon, 167, pp.148-159.

47. Li, J., Ma, W., Zhong, D., Li, K., Ma, J., Zhang, S., & Du, X. (2022). Oxygen vacancy concentration modulation of perovskite-based heterogeneous catalysts for Fenton-like oxidation of tetracycline. Journal of Cleaner Production, 362, 132469.

48. Liang, Q., Pan, D., & Zhang, X. (2022). Construction and application of biochar-based composite phase change materials. Chemical Engineering Journal, 139441

49. Lifšits, E. M., & Pitaevskij L. P. (1986). Elettrodinamica dei mezzi continui. Editori Riuniti Edizioni Mir.

50. Liu, Z., Zhao, N., Shi, C., He, F., Liu, E., & He, C. (2019). Synthesis of three-dimensional carbon networks decorated with Fe3O4 nanoparticles as lightweight and broadband electromagnetic wave absorber. Journal of Alloys and Compounds, 776, 691-701.

51. Liu, C., & Liao, X. (2020). Collagen fiber/Fe3O4/polypyrrole nanocomposites for absorption-type electromagnetic interference shielding and radar stealth. ACS Applied Nano Materials, 3(12), 11906-11915.

52. Liu, Y., Liu, Y., & Drew, M. G. (2021). A theoretical investigation on the quarter-wavelength model—part 1: analysis. Physica Scripta, 96(12), 125003.

53. Liu, Y., Liu, Y., & Drew, M. G. (2022). A theoretical investigation of the quarter-wavelength model-part 2: verification and extension. Physica Scripta, 97(1), 015806.

54. Lou, Z., Zhang, Y., Zhou, M., Han, H., Cai, J., Yang, L., Yuan, C., & Li, Y. (2018). Synthesis of magnetic wood fiber board and corresponding multi-layer magnetic composite board, with electromagnetic wave absorbing properties. Nanomaterials, 8(6), 441.

55. Lv, P., Xu, W., Li, D., Feng, Q., Yao, Y., Pang, Z., Lucia, L.A., & Wei, Q. (2016). Metal-based bacterial cellulose of sandwich nanomaterials for anti-oxidation electromagnetic interference shielding. Materials & Design, 112, 374-382.

56. Marins, J. A., Soares, B. G., Barud, H. S., & Ribeiro, S. J. (2013). Flexible magnetic membranes based on bacterial cellulose and its evaluation as electromagnetic interference shielding material. Materials Science and Engineering: C, 33(7), 3994-4001.

57. McMichael, R. D., Shull, R. D., Swartzendruber, L. J., Bennett, L. H., & Watson, R. E. (1992). Magnetocaloric effect in superparamagnets. Journal of Magnetism and Magnetic Materials, 111(1-2), 29-33.

58. Micheli, D., Apollo, C., Pastore, R., & Marchetti, M. (2010). X-Band microwave characterization of carbon-based nanocomposite material, absorption capability comparison and RAS design simulation. Composites Science and Technology, 70(2), 400-409.

59. Naito, Y., & Suetake, K. (1971). Application of ferrite to electromagnetic wave absorber and its characteristics. IEEE Transactions on Microwave Theory and Techniques, 19(1), 65-72.

60. Natalio, F., Corrales, T. P., Feldman, Y., Lew, B., & Graber, E. R. (2020). Sustainable lightweight biochar-based composites with electromagnetic shielding properties. ACS omega, 5(50), 32490-32497.

61. Ni, S., Lin, S., Pan, Q., Yang, F., Huang, K., & He, D. (2009). Hydrothermal synthesis and microwave absorption properties of Fe3O4 nanocrystals. Journal of Physics D: Applied Physics, 42(5), 055004.

62. Nikolopoulos, C. D., Baklezos, A. T., Kapetanakis, T. N., Vardiambasis, I. O., Tsubota, T., & Kalderis, D. (2023). Characterization of the Electromagnetic Shielding

Effectiveness of Biochar-Based Materials. IEEE Access, 11, 6413-6420.

63. Ok, Y. S., Uchimiya, S. M., Chang, S. X., & Bolan, N. (Eds.). (2015). Biochar: Production, characterization, and applications. CRC press

64. Pan, Y., Dai, M., Guo, Q., Yin, D., Zhuo, S., Hu, N., Yu, X., Hao, Y., & Huang, J. (2022). Multilayer wood/Cu-Fe3O4@Graphene/Ni composites for absorption-dominated electromagnetic shielding. Composite Interfaces, 29(6), 1-20.

65. Peng, F., Meng, F., Guo, Y., Wang, H., Huang, F., & Zhou, Z. (2018). Intercalating Hybrids of Sandwich-like Fe3O4–Graphite: Synthesis and Their Synergistic Enhancement of Microwave Absorption. ACS Sustain. Chem. Eng. 6, 16744–16753, DOI: 10.1021/acssuschemeng.8b04021

66. Poplavko, Y. (2021). Dielectric spectroscopy of electronic materials: Applied Physics of dielectrics. Woodhead Publishing.

67. Prokopchuk, A., Zozulia, I., Didenko, Y., Tatarchuk, D., Heuer, H., & Poplavko, Y. (2021). Dielectric permittivity model for polymer–filler composite materials by the example of Ni-and graphite-filled composites for high-frequency absorbing coatings. Coatings, 11(2), 172.

68. Qiang, C., Xu, J., Zhang, Z., Tian, L., Xiao, S., Liu, Y., & Xu, P. (2010). Magnetic properties and microwave absorption properties of carbon fibers coated by Fe3O4 nanoparticles. Journal of Alloys and Compounds, 506(1), 93-97.

69. Qin, M., Zhang, L., & Wu, H. (2022). Dielectric loss mechanism in electromagnetic wave absorbing materials. Advanced Science, 9(10), 2105553.

70. Qiu, X., Wang, L., Zhu, H., Guan, Y., & Zhang, Q. (2017). Lightweight and efficient microwave absorbing materials based on walnut shell-derived nano-porous carbon. Nanoscale, 9(22), 7408-7418.

71. Ramo, S., Whinnery, J.R., & Van Duzer, T. ()1994). Fields and waves in communications electronics. JohnWiley and Son.

72. Ruiz-Perez, F., López-Estrada, S. M., Tolentino-Hernández, R. V., & Caballero-Briones, F. (2022). Carbon-based, radar absorbing materials: A critical review. Journal of Science: Advanced Materials and Devices, 100454.

73. Sabu, T., Kuruvilla, J., Malhotra, S. K., Goda, K., & Sreekala, M. K. (2012). Polymer Composites, Macro-and Microcomposites. Weinheim, Germany: John Wiley & Sons, 1, 356-358.

74. Saini, P., Choudhary, V., Vijayan, N., & Kotnala, R. K. (2012). Improved electromagnetic interference shielding response of poly (aniline)-coated fabrics containing dielectric and magnetic nanoparticles. The Journal of Physical Chemistry C, 116(24), 13403-13412.

75. Savi, P., Yasir, M., Bartoli, M., Giorcelli, M., & Longo, M. (2020). Electrical and microwave characterization of thermal annealed sewage sludge derived biochar composites. Applied Sciences, 10(4), 1334–1345.

76. Shen, R., Weng, M., Zhang, L., Huang, J., & Sheng, X. (2022). Biomass-based carbon aerogel/Fe3O4@ PEG phase change composites with satisfactory electromagnetic interference shielding and multi-source driven thermal management in thermal energy storage. Composites Part A: Applied Science and Manufacturing, 163, 107248.

77. Singh, K., Ohlan, A., Pham, V.H., Balasubramaniyan, R., Varshney, S., Jang, J., Hur, S.H., Choi, W.M., Kumar, M., Dhawan, S.K., & Kong, B.S. (2013). Nanostructured graphene/Fe 3 O 4 incorporated polyaniline as a high performance shield against electromagnetic pollution. Nanoscale, 5(6), 2411-2420.

78. Singh, R., & Bhateria, R. (2021). Core–shell nanostructures: a simplest two-component system with enhanced properties and multiple applications. Environmental Geochemistry and Health, 43, 2459-2482.

79. Singhal, S. (2022). Biochar as a cost-effective and eco-friendly substitute for binder in concrete: a review. European Journal of Environmental and Civil Engineering, 1-26.

80. Soares, B. G., Barra, G. M., & Indrusiak, T. (2021). Conducting polymeric composites based on intrinsically conducting polymers as electromagnetic interference shielding/microwave absorbing materials—A review. Journal of Composites Science, 5(7), 173.

81. Sparavigna, A., Henn, A. R., & Florio, L. (2005). Textiles as electromagnetic shields for human and device safety. Applied Physics, Recent Res. Develop., 1-20.

82. Sparavigna, A. C. (2022). Biochar for Shape Stabilized Phase-Change Materials . ChemRxiv. Cambridge: Cambridge Open Engage; 2022. https://doi.org/10.26434/chemrxiv-2022-4nthj

83. Sparavigna A. C. (2023). Iron Oxide Fe3O4 Nanoparticles for Electromagnetic Shielding. ChemRxiv. Cambridge: Cambridge Open Engage; 2023. https://doi.org/10.26434/chemrxiv-2023-g9bkz-v2

84. Sparavigna, A. C. Iron Oxide Fe3O4 Nanoparticles with ICPs and Biochar to Improve Electromagnetic Shielding Performance (February 23, 2023). Available at SSRN: https://ssrn.com/abstract=4331866 or http://dx.doi.org/10.2139/ssrn.4331866

85. Sparavigna, A. C. (2023). Multifunctional porosity in biochar. International Journal of Sciences, 12(07), 41-54. DOI: 10.18483/ijSci.2694

86. Tong, S., Zhu, H., & Bao, G. (2019). Magnetic iron oxide nanoparticles for disease detection and therapy. Materials Today, 31, 86-99.

87. Torsello, D., Bartoli, M., Giorcelli, M., Rovere, M., Arrigo, R., Malucelli, G., Tagliaferro, A., & Ghigo, G. (2021). High frequency electromagnetic shielding by biochar-based composites. Nanomaterials, 11(9), p.2383.

88. Wallyn, J., Anton, N., & Vandamme, T. F. (2019). Synthesis, principles, and properties of magnetite nanoparticles for in vivo imaging applications—A review. Pharmaceutics, 11(11), 601.

89. Wang, B., Wei, J., Yang, Y., Wang, T., & Li, F. (2011). Investigation on peak frequency of the microwave absorption for carbonyl iron/epoxy resin composite. Journal of Magnetism and Magnetic Materials, 323(8), 1101-1103.

90. Wang, H., Meng, F., Li, J., Li, T., Chen, Z., Luo, H., & Zhou, Z. (2018). Carbonized design of hierarchical porous carbon/Fe3O4@ Fe derived from loofah sponge to achieve tunable high-performance microwave absorption. ACS Sustainable Chemistry & Engineering, 6(9), 11801-11810.

91. Wang, L., Guan, H., Hu, J., Huang, Q., Dong, C., Qian, W., & Wang, Y. (2019). Jute-based porous biomass carbon composited by Fe3O4 nanoparticles as an excellent microwave absorber. Journal of Alloys and Compounds, 803, 1119-1126.

92. Wang, H., Zhang, Y., Wang, Q., Jia, C., Cai, P., Chen, G., Dong, C., & Guan, H. (2019). Biomass carbon derived from pine nut shells decorated with NiO nanoflakes for enhanced microwave absorption properties. RSC advances, 9(16), 9126-9135.

93. Wang, L., Li, X., Shi, X., Huang, M., Li, X., Zeng, Q., & Che, R. (2021). Recent progress of microwave absorption microspheres by magnetic–dielectric synergy. Nanoscale, 13(4), 2136-2156.

94. Wang, L., Guan, H., Su, S., Hu, J., & Wang, Y. (2022). Magnetic FeOX/biomass carbon composites with broadband microwave absorption properties. Journal of Alloys and Compounds, 903, 163894.

95. Wang, Q., Wu, X., Huang, J., Chen, S., Zhang, Y., Dong, C., Chen, G., Wang, L., & Guan, H. (2022). Enhanced microwave absorption of biomass carbon/nickel/polypyrrole (C/Ni/PPy) ternary composites through the synergistic effects. Journal of Alloys and Compounds, 890, 161887.

96. Wang, L., Su, S., & Wang, Y. (2022). Fe3O4–Graphite Composites as a Microwave Absorber with Bimodal Microwave Absorption. ACS Applied Nano Materials, 5(12), 17565-17575.

97. Wang, Y., Wan, S., Yu, W., Yuan, D., & Sun, L. (2022). The role of Fe3O4@ biochar as electron shuttle in enhancing the biodegradation of gaseous para-xylene by aerobic surfactant secreted strains. Journal of Hazardous Materials, 438, 129475.

98. Wei, J., Liu, J., & Li, S. (2007). Electromagnetic and microwave absorption properties of Fe3O4 magnetic films plated on hollow glass spheres. Journal of magnetism and magnetic materials, 312(2), 414-417.

99. Wei, Y., Han, B., Hu, X., Lin, Y., Wang, X., & Deng, X. (2012). Synthesis of Fe3O4 nanoparticles and their magnetic properties. Procedia Engineering, 27, 632-637.

100. Wen, F. S., Zhang, F., & Liu, Z. Y. (2011). Investigation on Microwave Absorption Properties for Multiwalled Carbon Nanotubes/Fe/Co/Ni Nanopowders as Lightweight Absorbers. J. Phys. Chem. C 2011, 115, 14025-14030.

101. Wu, Z., Tan, D., Tian, K., Hu, W., Wang, J., Su, M., & Li, L. (2017). Facile preparation of core–shell Fe3O4@ Polypyrrole composites with superior electromagnetic wave absorption properties. The Journal of Physical Chemistry C, 121(29), 15784-15792.

102. Wu, Z., Tian, K., Huang, T., Hu, W., Xie, F., Wang, J., Su, M., & Li, L. (2018). Hierarchically porous carbons derived from biomasses with excellent microwave absorption performance. ACS applied materials & interfaces, 10(13), pp.11108-11115.

103. Xu, F., Ma, L., Huo, Q., Gan, M., & Tang, J. (2015). Microwave absorbing properties and structural design of microwave absorbers based on polyaniline and polyaniline/magnetite nanocomposite. Journal of Magnetism and Magnetic Materials, 374, 311-316.

104. Yang, H., Chao, W., Di, X., Yang, Z., Yang, T., Yu, Q., Liu, F., Li., J., Li, G. , & Wang, C. (2019). Multifunctional wood based composite phase change materials for magnetic-thermal and solar-thermal energy conversion and storage. Energy Conversion and Management, 200, 112029.

105. Yan, F., Xue, G., Chen, J., & Lu, Y. (2001). Preparation of a conducting polymer/ferromagnet composite film by anodic-oxidation method. Synthetic metals, 123(1), 17-20.

106. Yang, F., Hou, X., Wang, L., Li, Y., & Yu, M. (2020). Preparation of Ferrite Fe3O4 and Its Electromagnetic Wave Absorption Properties. In IOP Conference Series: Materials Science and Engineering (Vol. 772, No. 1, p. 012115). IOP Publishing.

107. Yao, Y., Miao, S., Liu, S., Ma, L. P., Sun, H., & Wang, S. (2012). Synthesis, characterization, and adsorption properties of magnetic Fe3O4@ graphene nanocomposite. Chemical engineering journal, 184, 326-332.

108. Yasir, M., Di Summa, D., Ruscica, G., Natali Sora, I., & Savi, P. (2020). Shielding properties of cement composites filled with commercial biochar. Electronics, 9(5), 819.

109. Yin, P., Zhang, L., Wang, J., Feng, X., Dai, J., & Tang, Y. (2021). Facile preparation of cotton-derived carbon fibers loaded with hollow Fe3O4 and CoFe NPs for significant low-frequency electromagnetic absorption. Powder Technology, 380, 134-142.

110. Yin, P., Zhang, L., Jiang, Y., Zhang, Y., Wang, J., Feng, X., Dai, J., & Tang, Y. (2020). Recycling of waste straw in sorghum for preparation of biochar/(Fe, Ni) hybrid aimed at significant electromagnetic absorbing of low-frequency band. Journal of Materials Research and Technology, 9(6), 14212-14222.

111. Yörük, A. E., Erdoğan, M. K., Karakışla, M., & Saçak, M. (2021). Deposition of electrically-conductive polyaniline/ferrite nanoparticles onto the polypropylene nonwoven for the development of an electromagnetic interference shield material. The Journal of The Textile Institute, 1-13.

112. Yusoff, A. N., Abdullah, M. H., Ahmad, S. H., Jusoh, S. F., Mansor, A. A., & Hamid, S. A. A. (2002). Electromagnetic and absorption properties of some microwave absorbers. Journal of Applied Physics, 92(2), 876-882.

113. Zhao, H., Cheng, Y., Liu, W., Yang, L., Zhang, B., Wang, L.P., Ji, G., & Xu, Z.J. (2019). Biomass-derived porous carbon-based nanostructures for microwave absorption. Nano-Micro Letters, 11(1), 1-17.

114. Zheng, X., Tang, J., Cheng, L., Yang, H., Zou, L., & Li, C. (2023). Superhydrophobic hollow magnetized Fe3O4 nanospheres/MXene fabrics for electromagnetic interference shielding. Journal of Alloys and Compounds, 934, 167964.

115. Zhou, X., Jia, Z., Feng, A., Wang, X., Liu, J., Zhang, M., Cao, H., & Wu, G. (2019). Synthesis of fish skin-derived 3D carbon foams with broadened bandwidth and excellent electromagnetic wave absorption performance. Carbon, 152, 827-836.

116. Ziegler, D., Francia, E. D., Savi, P., & Tulliani, J. M. (2020). Biochar addition to inorganic binders. In Biochar: Emerging applications (pp. 11-1). Bristol, UK: IOP Publishing.